located in this partner-factor interaction region, which is important for the cell-specific actions of SOX2. Missense mutations in this region may lead to phenotypic variability in ocular malformation and/or HH due not only to residual SOX2 activity, but also the interaction with tissue-specific partner factors.

We used a next-generation sequencing strategy to analyze 122 genes associated with congenital endocrine disorders. This approach is new in HH; it has never been reported to our knowledge. The genetic etiologies of HH are quite heterogeneous, and recent investigations have revealed that HH is not strictly a monogenic mendelian disease as previously thought; instead, it is emerging as a digenic and potentially oligogenic disease [17, 18]. When multiple genes need to be analyzed for mutations simultaneously, targeted sequence analysis of interesting genomic regions is an attractive approach.

In summary, this study expands the range of known molecular defects in SOX2, and extends our understanding of the phenotypic features and developmental disease course associated with mutations in *SOX2*.

Acknowledgments

We thank Kazue Kinoshita for technical assistance. We also thank Professor Takao Takahashi for his fruitful discussion of our study. This work was supported by Health and Labour Sciences Research Grant for Research on Applying Health Technology [Jitsuyoka (Nanbyo) – Ippan-014].

Disclosure Statement

The authors have nothing to disclose.

References

1 Karges B, de Roux N: Molecular genetics of isolated hypogonadotropic hypogonadism and Kallmann syndrome. Endocr Dev 2005;8:67–80.
2 de Roux N: GnRH receptor and GPR54 inactivation in isolated gonadotropic deficiency. Best Pract Res Clin Endocrinol Metab 2006; 20:515–528.
3 Silveira LF, Trarbach EB, Latronico AC: Genetics basis for GnRH-dependent pubertal disorders in humans. Mol Cell Endocrinol 2010;324:30–38.
4 Bouligand J, Ghervan C, Tello JA, Brailly-Tabard S, Salenave S, Chanson P, Lombès M, Millar RP, Guiochon-Mantel A, Young J: Isolated familial hypogonadotropic hypogonadism and a GNRH1 mutation. N Engl J Med 2009;360:2742–2748.
5 Topaloglu AK, Reimann F, Guclu M, Yalin AS, Kotan LD, Porter KM, Serin A, Mungan NO, Cook JR, Ozbek MN, Imamoglu S, Akalin NS, Yuksel B, O'Rahilly S, Semple RK: TAC3 and TACR3 mutations in familial hypogonadotropic hypogonadism reveal a key role for neurokinin B in the central control of reproduction. Nat Genet 2009;41:354–358.
6 Topaloglu AK, Tello JA, Kotan LD, Ozbek MN, Yilmaz MB, Erdogan S, Gurbuz F, Temiz F, Millar RP, Yuksel B: Inactivating KISS1 mutation and hypogonadotropic hypogonadism. N Engl J Med 2012;366:629–635.
7 Kelberman D, Rizzoti K, Avilion A, Bitner-Glindzicz M, Cianfarani S, Collins J, Chong WK, Kirk JM, Achermann JC, Ross R, Carmignac D, Lovell-Badge R, Robinson IC, Dattani MT: Mutations within Sox2/SOX2 are associated with abnormalities in the hypothalamo-pituitary-gonadal axis in mice and humans. J Clin Invest 2006;116:2442–2455.
8 Kelberman D, de Castro SC, Huang S, Crolla JA, Palmer R, Gregory JW, Taylor D, Cavallo L, Faienza MF, Fischetto R, Achermann JC, Martinez-Barbera JP, Rizzoti K, Lovell-Badge R, Robinson IC, Gerrelli D, Dattani MT: SOX2 plays a critical role in the pituitary, forebrain, and eye during human embryonic development. J Clin Endocrinol Metab 2008; 93:1865–1873.
9 Fantes J, Ragge NK, Lynch SA, McGill NI, Collin JR, Howard-Peebles PN, Hayward C, Vivian AJ, Williamson K, van Heyningen V, FitzPatrick DR: Mutations in SOX2 cause anophthalmia. Nat Genet 2003;33:461–463.
10 Williamson KA, Hever AM, Rainger J, Rogers RC, Magee A, Fiedler Z, Keng WT, Sharkey FH, McGill N, Hill CJ, Schneider A, Messina M, Turnpenny PD, Fantes JA, van Heyningen V, FitzPatrick DR: Mutations in SOX2 cause anophthalmia-esophageal-genital (AEG) syndrome. Hum Mol Genet 2006; 15:1413–1422.
11 Schneider A, Bardakjian T, Reis LM, Tyler RC, Semina EV: Novel SOX2 mutations and genotype-phenotype correlation in anophthalmia and microphthalmia. Am J Med Genet A 2009;149A:2706–2715.
12 Leiden University Medical Center. Leiden Open Variation Database. MRC Human Genetics Unit LOVD at MRC IGMM. Leiden University Medical Center website. http://lsdb.hgu.mrc.ac.uk/home.php.
13 Woods KS, Cundall M, Turton J, Rizotti K, Mehta A, Palmer R, Wong J, Chong WK, Al-Zyoud M, El-Ali M, Otonkoski T, Martinez-Barbera JP, Thomas PQ, Robinson IC, Lovell-Badge R, Woodward KJ, Dattani MT: Over- and underdosage of SOX3 is associated with infundibular hypoplasia and hypopituitarism. Am J Hum Genet 2005;76:833–849.
14 Sato N, Kamachi Y, Kondoh H, Shima Y, Morohashi K, Horikawa R, Ogata T: Hypogonadotropic hypogonadism in an adult female with a heterozygous hypomorphic mutation of SOX2. Eur J Endocrinol 2007;156:167–171.
15 Mihelec M, Abraham P, Gibson K, Krowka R, Susman R, Storen R, Chen Y, Donald J, Tam PP, Grigg JR, Flaherty M, Gole GA, Jamieson RV: Novel SOX2 partner-factor domain mutation in a four-generation family. Eur J Hum Genet 2009;17:1417–1422.
16 Kamachi Y, Cheah KS, Kondoh H: Mechanism of regulatory target selection by the SOX high-mobility-group domain proteins as revealed by comparison of SOX1/2/3 and SOX9. Mol Cell Biol 1999;19:107–120.
17 Pitteloud N, Durrani S, Raivio T, Sykiotis GP: Complex genetics in idiopathic hypogonadotropic hypogonadism. Front Horm Res 2010; 39:142–153.
18 Sykiotis GP, Plummer L, Hughes VA, Au M, Durrani S, Nayak-Young S, Dwyer AA, Quinton R, Hall JE, Gusella JF, Seminara SB, Crowley WF Jr, Pitteloud N: Oligogenic basis of isolated gonadotropin-releasing hormone deficiency. Proc Natl Acad Sci USA 2010;34: 15140–15144.

3 Lang GH, Kagiya Y, Ohnishi-Kameyama M, Kitta K. Evaluation of extraction solutions for biochemical analyses of the proteins in rice grains. *Biosci. Biotechnol. Biochem.* 2013; **77**: 126–31.
4 Urisu A, Yamada K, Masuda S *et al.* 16-kilodalton rice protein is one of the major allergens in rice grain extract and responsible for cross-allergenicity between cereal grains in the Poaceae family. *Int. Arch. Allergy Appl. Immunol.* 1991; **96**: 244–52.
5 Usui Y, Nakase M, Hotta H *et al.* A 33-kDa allergen from rice (Oryza sativa L. Japonica). cDNA cloning, expression, and identification as a novel glyoxalase I. *J. Biol. Chem.* 2001; **276**: 11376–81.
6 Asero R, Amato S, Alfieri B, Folloni S, Mistrello G. Rice: Another potential cause of food allergy in patients sensitized to lipid transfer protein. *Int. Arch. Allergy Immunol.* 2007; **143**: 69–74.
7 Ikezawa Z, Tsubaki K, Osuna H *et al.* [Usefulness of hypoallergenic rice (AFT-R 1) and analysis of the salt insoluble rice allergen molecule]. *Arerugi* 1999; **48**: 40–9.
8 Kilshaw PJ, Heppell LM, Ford JE. Effects of heat treatment of cow's milk and whey on the nutritional quality and antigenic properties. *Arch. Dis. Child.* 1982; **57**: 842–7.
9 Sasagawa A, Yamazaki A. Development of food products using high-pressure induced transformation (Hi-pit). *Rev. High Pressure Sci. Technol.* 2008; **18**: 139–46.

Neonatal case of classic maple syrup urine disease: Usefulness of ^{1}H-MRS in early diagnosis

Takeshi Sato,[1,5] Koji Muroya,[1] Junko Hanakawa,[1] Yumi Asakura,[1] Noriko Aida,[2] Moyoko Tomiyasu,[3] Go Tajima,[4] Tomonobu Hasegawa[5] and Masanori Adachi[1]

Departments of [1]Endocrinology and Metabolism and [2]Radiology, Kanagawa Children's Medical Center, Yokohama, [3]Research Center for Charged Particle Therapy, National Institute of Radiological Sciences, Chiba, [4]Department of Pediatrics, Hiroshima University Graduate School of Biomedical and Health Sciences, Hiroshima and [5]Department of Pediatrics, Keio University School of Medicine, Tokyo, Japan

Abstract We describe a male neonate with classic maple syrup urine disease (MSUD) in metabolic crisis. On day 7 of life, he was referred to hospital because of coma and metabolic acidosis with maple syrup odor. On day 4 after admission, brain magnetic resonance imaging findings were consistent with encephalopathy due to MSUD. Proton magnetic resonance spectroscopy (^{1}H-MRS) showed a large methyl resonance peak at 0.9 p.p.m. The diagnosis of MSUD was confirmed on low branched-chain α-keto acid dehydrogenase complex activity in lymphocyte. ^{1}H-MR spectra were obtained in 10 min, while it took at least several days to obtain the results of other diagnostic examinations. In convalescence, the peak at 0.9 p.p.m. decreased. The large methyl resonance peak at 0.9 p.p.m. in brain ^{1}H-MRS would be one of the earliest clues to the diagnosis of classic MSUD in the neonatal period, especially in metabolic crisis.

Key words early diagnosis, maple syrup urine disease, metabolic crisis, neonate, proton magnetic resonance spectroscopy.

Maple syrup urine disease (MSUD; OMIM 248600) is a rare autosomal recessive inborn error of branched-chain amino acid (BCAA) metabolism.[1] The defect of the branched-chain α-keto acid dehydrogenase complex leads to the accumulation of BCAA, including leucine, valine and isoleucine, and their α-keto acids in tissues. Clinical manifestations include a maple syrup odor, mental and motor retardation, feeding problems, and convulsion. Laboratory findings include metabolic ketoacidosis, elevated plasma leucine, valine and isoleucine, sometimes hypoglycemia, hyperlactatemia and hyperammonemia. In metabolic crisis, fatal brain edema sometimes occurs. MSUD is divided into five different forms: classic; intermittent; intermediate; thiamine responsive; and dihydrolipoyl dehydrogenase (E3) deficient.

Some neonates with classic MSUD suffer from metabolic crisis within 1 week after birth,[1] before neonatal screening results are obtained. Although early diagnosis and specific treatment improve the outcome in neonates with classic MSUD,[2] it is challenging to diagnose MSUD early for two reasons. First, it is difficult for pediatricians to distinguish MSUD from common fatal diseases in the neonatal period, because patients with MSUD do not show any specific clinical manifestations except a maple syrup odor, nor specific routine laboratory findings. Second, it takes at least several days to obtain the results of diagnostic examinations, because most pediatricians cannot perform diagnostic examinations in their own laboratories.

Correspondence: Koji Muroya, MD PhD, Department of Endocrinology and Metabolism, Kanagawa Children's Medical Center, 2-138-4 Mutsukawa, Minami-ku, Yokohama-shi, Kanagawa 232-8555, Japan. Email: kmuroya@kcmc.jp

Received 5 April 2013; revised 22 July 2013; accepted 9 August 2013.
doi: 10.1111/ped.12211

Proton magnetic resonance spectroscopy (^{1}H-MRS) directly and non-invasively measures regional metabolite levels *in vivo*. One ^{1}H-MRS datum can be obtained within 10 min, in addition to routine magnetic resonance imaging (MRI) of the brain. ^{1}H-MRS has been applied to provide additional information for radiological diagnosis of neurodegenerative disorders, brain tumors and metabolic diseases.[3,4] In previous studies, ^{1}H-MR spectra in older children with MSUD had a methyl resonance peak at 0.9 p.p.m. that increased remarkably in metabolic decompensation.[5–7] Although there is one report on ^{1}H-MRS in neonates with classic MSUD in metabolic crisis,[5] the potential benefit of ^{1}H-MRS in early diagnosis of classic MSUD has not been discussed.

Here, we focus on the usefulness of ^{1}H-MRS in early diagnosis of classic MSUD in the neonatal period, especially in metabolic crisis.

Case report

The proband, a male neonate, was the fourth child of healthy, non-consanguineous Filipino parents. An elder sister died due to metabolic crisis of MSUD at 9 years of age. The proband was delivered vaginally at term. His birthweight was 3724 g (+1.7 SD), length, 50.0 cm (+0.4 SD), and head circumference, 36.0 cm (+2.0 SD). He had been breastfed. He left the hospital on day 4 of life with his mother.

His parents noticed poor feeding and a maple syrup odor on day 6 of life. The previous doctor referred him to hospital due to metabolic acidosis on day 7 of life. On clinical examination he was in a comatose state with a bulging anterior fontanelle. Blood tests indicated normal ammonia level (72 μmol/L; reference, <110 μmol/L). Computed tomography indicated brain edema. We suspected that he suffered from metabolic crisis of MSUD based on family history and the maple syrup odor. On day 2 after admission, we started a BCAA-free formula. On day 4 after admission, MRI of the brain at 3 T showed marked restriction of proton diffusion in the thalami, the posterior limb of the internal capsule and the globus pallidus (Fig. 1a,b). In addition, ^{1}H-MR spectra showed a large methyl peak at 0.9 p.p.m., at the left centrum–semiovale and the left basal ganglia that were obtained in 5 min each (Fig. 1c,d). A decreased *N*-acetyl aspartate (NAA) peak was also observed (Fig. 1c,d). These findings were consistent with MSUD encephalopathy. We obtained the results of neonatal screening the next day and other diagnostic examinations the next week (Table 1). The diagnosis of MSUD was confirmed by low branched-chain α-keto acid dehydrogenase complex

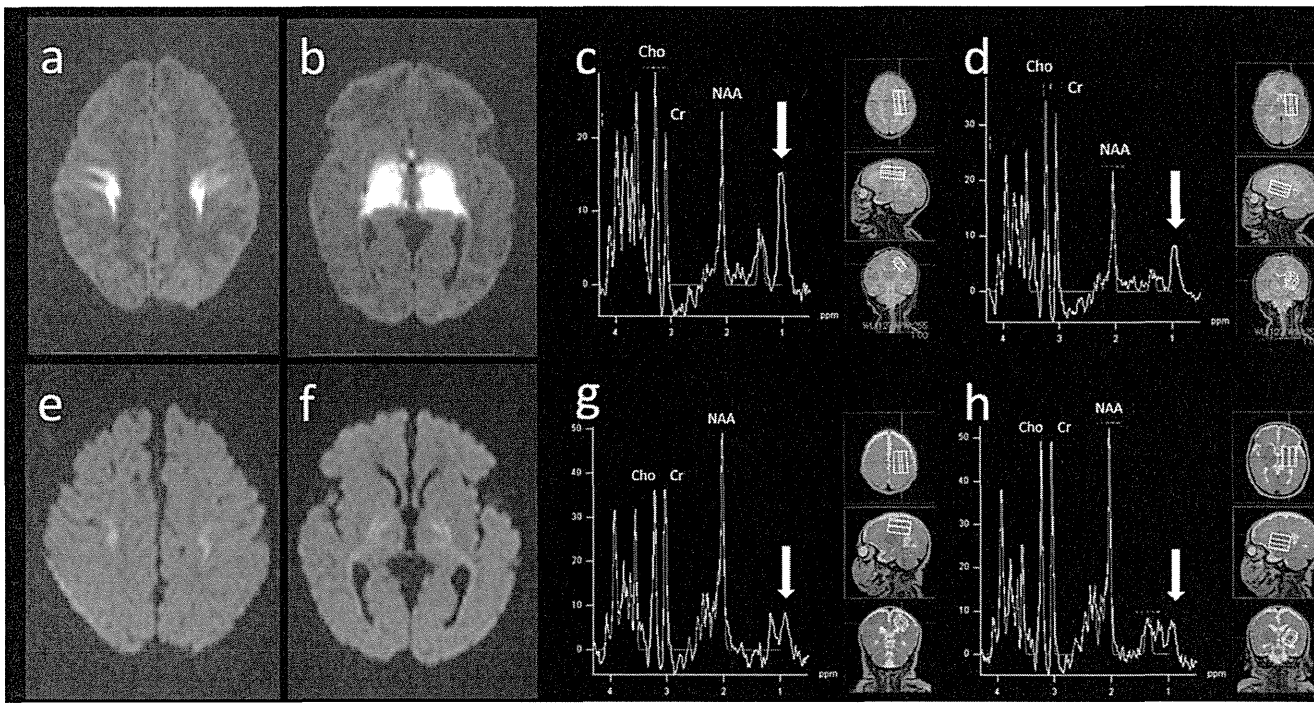

Fig. 1 Magnetic resonance imaging and proton magnetic resonance spectroscopy (^{1}H-MRS) findings at (a–d) onset and in (e–h) convalescence. (a,b) Axial diffusion-weighted images (TR/TE, 6700/123 ms; section thickness, 3.0 mm; b value, 1500 s/mm^2) at (a) centrum–semiovale and (b) internal capsule. Note marked restriction of proton diffusion in the thalami, the posterior limb of the internal capsule and the globus pallidus. (c,d) ^{1}H-MRS (TR/TE/NEX, 5000 ms/30 ms/6) at (c) the left centrum–semiovale and (d) the left basal ganglia. Note the large peak at 0.9 p.p.m. (arrows) and the decreased NAA peak. (e,f) Axial diffusion-weighted images (TR/TE, 7200/120 ms; section thickness, 3.0 mm; b value, 1500 s/mm^2) at (e) centrum–semiovale and (f) internal capsule. Note the significant resolution of the hyperintense lesions. (g,h) ^{1}H-MRS (TR/TE/NEX, 5000 ms/30 ms/6) at (g) the left centrum–semiovale and (h) the left basal ganglia. Note the decreased peak at 0.9 p.p.m. (arrows) and the increased NAA peak. The Cr level in convalescence was higher than the one at the onset. Cho, choline; Cr, creatine; NAA, *N*-acetyl aspartate; NEX, no. excitations; TE, echo time; TR, repetition time.

Table 1 Diagnostic examinations

Diagnostic examinations		Results (local references)		Time required for results
Neonatal screening by high performance liquid chromatography	Leucine	21.1 (<3.5)	mg/dL	7 days
Plasma amino acid analysis by liquid chromatography mass spectrometry	Leucine	3218.6 (76.6–171.3)	nmol/mL	12 days
	Valine	1076.1 (147.8–307.0)	nmol/mL	
	Isoleucine	1000.4 (43.0–112.8)	nmol/mL	
Urine organic acid analysis	High levels of α-keto and hydroxyl acids			13 days
Branched-chain α-keto acid dehydrogenase complex activity in lymphocyte	0.14 (3.89–7.43)	pmol isovaleryl-CoA/min/10^6 lymphocytes		3 days

activity in lymphocyte (Table 1). In spite of intensive treatment with BCAA-free formula through the nasogastric tube and parenteral high-caloric nutrition with insulin, he developed a high ammonia level (218 μmol/L) and needed continuous arteriovenous hemofiltration on day 24 after admission. He then made satisfactory progress. In convalescence at 2 months of age, MRI indicated significant resolution of the hyperintense lesions (Fig. 1e,f). On ^{1}H-MRS the peak at 0.9 p.p.m. had decreased and the NAA peak had increased (Fig. 1g,h; Table 2). The creatine (Cr) level in convalescence was higher than that at onset (Fig. 1; Table 2). On day 157 after admission, he left hospital, using the nasogastric tube. He managed to drink milk from a bottle at 6 months of age. He started babbling and pulling himself up at 16 months of age.

Discussion

We have described a male neonate with classic MSUD in metabolic crisis. Based on his family history and the maple syrup odor, we started BCAA-free formula, before we obtained the results of other diagnostic examinations. Brain ^{1}H-MRS showed a large methyl resonance peak at 0.9 p.p.m. characteristic for MSUD, at the left centrum–semiovale and the left basal ganglia in 5 min each. In contrast, it took at least several days to obtain the results of other diagnostic examinations, including neonatal screening, plasma amino acid analysis, urine organic acid analysis and enzymatic activity. Retrospectively, we believe that the large methyl resonance peak at 0.9 p.p.m. on brain ^{1}H-MRS would be one of the earliest clues to the diagnosis of classic MSUD in the neonatal period, especially in metabolic crisis.

In MSUD the peak at 0.9 p.p.m. is larger than the one at 1.3 p.p.m. on ^{1}H-MRS of the brain. In MSUD patients, the large peak at 0.9 p.p.m. is thought to originate from BCAA and/or their derivatives, which have more methyl groups (-CH_3 at 0.9 p.p.m.) than methylene groups (-CH_2- at 1.3 p.p.m.).[7] We must interpret the peaks at 0.9 p.p.m. and 1.3 p.p.m. with caution, because the resonance at 0.9 p.p.m. and 1.3 p.p.m. is not specific to MSUD. Several disorders, such as Sjögren–Larsson syndrome, have prominent lipid peaks at both 0.9 p.p.m. and 1.3 p.p.m.[8] Hyperlactatemia, which often occurs in metabolic crisis of MSUD, can also be confused with the peak at 1.3 p.p.m. Fortunately, it is not difficult to exclude other diseases based on medical history, physical examinations and routine laboratory examinations.

We could not determine whether the NAA and Cr levels increased in convalescence due to therapeutic response or to age-dependent changes (Table 2). NAA is considered to be a marker of neuronal density or mitochondrial metabolic function.[9] A decreased NAA peak could be observed in metabolic disorders.[4] It is also well known, however, that NAA concentration increases with development.[10] Cr level is reported to be relatively stable, but may change with development or tissue damage.[4] We observed that the choline (Cho) level remained almost unchanged (Table 2). Although Cho is known to be involved in cell membrane metabolism and myelination,[4] the significance of the Cho level remained unknown in MSUD. In contrast, the decreased peak at 0.9 p.p.m. might have reflected decreased BCAA and/or their α-keto acids directly. ^{1}H-MRS in the present neonatal patient showed a decreased peak at 0.9 p.p.m. in convalescence at 2 months of age, compared with the one at onset (Fig. 1; Table 2). Previous studies showed that the peak at 0.9 p.p.m. decreased in convalescence in older children.[5] Thus, among the peaks of the major metabolites, such as NAA, Cr and Cho, the peak at 0.9 p.p.m. would be the most useful to estimate the efficacy of treatment regardless of patient age.

Conclusion

We have demonstrated the usefulness of ^{1}H-MRS at the centrum-semiovale and the basal ganglia in early diagnosis of classic

Table 2 Metabolite concentrations

	-CH_3 (at 0.9 p.p.m.)†		*N*-acetyl aspartate		Choline		Creatine	
	CS	BG	CS	BG	CS	BG	CS	BG
Onset (mmol/L)	11.3	6.3	2.7	2.7	1.3	1.9	3.4	5.1
Convalescence (mmol/L)	6.0	4.9	4.8	5.1	1.5	1.8	5.5	6.8

Quantification of metabolite concentrations were derived using LCModel software. †mmol/L of CH_3 groups. BG, basal ganglia; CS, centrum–semiovale.

MSUD in the neonatal period, especially in metabolic crisis. Classic MSUD may be able to be distinguished from other serious illnesses and specific treatment initiated immediately, when ^{1}H-MRS findings are interpreted in combination with the clinical course, physical examinations, routine laboratory findings and routine MRI findings.

Acknowledgments

We thank the family for participating in this study. We also thank Drs Takahiro Murata and Akira Ishiguro for providing us with clinical information, and Dr Satoshi Narumi for fruitful discussion and critical reading of the manuscript.

References

1 Morton DH, Strauss KA, Robinson DL, Puffenberger EG, Kelley RI. Diagnosis and treatment of maple syrup disease: A study of 36 patients. *Pediatrics* 2002; **109**: 999–1008.
2 Naughten ER, Jenkins J, Francis DE, Leonard JV. Outcome of maple syrup urine disease. *Arch. Dis. Child.* 1982; **57**: 918–21.
3 Wang Z, Zimmerman RA, Sauter R. Proton MR spectroscopy of the brain: Clinically useful information obtained in assessing CNS diseases in children. *AJR Am. J. Roentgenol.* 1996; **167**: 191–9.
4 Wang ZJ, Zimmerman RA. Proton MR spectroscopy of pediatric brain metabolic disorders. *Neuroimaging Clin. N. Am.* 1998; **8**: 781–807.
5 Jan W, Zimmerman RA, Wang ZJ, Berry GT, Kaplan PB, Kaye EM. MR diffusion imaging and MR spectroscopy of maple syrup urine disease during acute metabolic decompensation. *Neuroradiology* 2003; **45**: 393–9.
6 Felber SR, Sperl W, Chemelli A, Murr C, Wendel U. Maple syrup urine disease: Metabolic decompensation monitored by proton magnetic resonance imaging and spectroscopy. *Ann. Neurol.* 1993; **33**: 396–401.
7 Heindel W, Kugel H, Wendel U, Roth B, Benz-Bohm G. Proton magnetic resonance spectroscopy reflects metabolic decompensation in maple syrup urine disease. *Pediatr. Radiol.* 1995; **25**: 296–9.
8 Tachibana Y, Aida N, Enomoto K, Iai M, Kurosawa K. A case of Sjögren-Larsson syndrome with minimal MR imaging findings facilitated by proton spectroscopy. *Pediatr. Radiol.* 2012; **42**: 380–82.
9 Govindaraju V, Young K, Maudsley AA. Proton NMR chemical shifts and coupling constants for brain metabolites. *NMR Biomed.* 2000; **13**: 129–53.
10 Kreis R, Hofmann L, Kuhlmann B, Boesch C, Bossi E, Hüppi PS. Brain metabolite composition during early human brain development as measured by quantitative in vivo ^{1}H magnetic resonance spectroscopy. *Magn. Reson. Med.* 2002; **48**: 949–58.

Two children with obesity-related glomerulopathy identified in a school urinary screening program

Yukihiko Kawasaki, Masato Isome, Atsushi Ono, Yuichi Suzuki, Kei Takano, Kazuhide Suyama and Mitsuaki Hosoya
Department of Pediatrics, Fukushima Medical University School of Medicine, Fukushima, Japan

Abstract The incidence of obesity-related glomerulopathy (ORG) has increased over the last decade, but there have been few reports on ORG in Japanese children. Reported herein are two children with ORG identified on school urinary screening (SUS). Patient 1 was a 12-year-old boy in whom proteinuria was first detected on SUS. His body mass index (BMI) was 33.8 kg/m^2 and he had hypertension and hyperuricemia. Patient 2, a 10-year-old boy, also had proteinuria identified on SUS. His BMI was 34.8 kg/m^2, and he had fatty liver, hyperuricemia, and hypercholesterolemia. Both were diagnosed with ORG based on obesity, proteinuria, and renal pathological findings. After treatment, including candesartan, food restriction and physical exercise, urinary protein excretion was decreased in both cases. We believe that such school urinary screening programs may be effective for the early identification and treatment of children with ORG.

Key words angiotensin II receptor blocker child, focal segmental glomerulosclerosis, obesity-related glomerulopathy, school urinary screening.

Obesity is a major health problem, and its incidence is increasing worldwide.[1] In Japan, the prevalence of obesity has been consistently increasing in men, whereas it has been stable over the last 10 years in women: according to the annual report of the National Nutrition Survey, Japan, currently, the prevalence of overweight is 30.9% in men and 22.7% in women aged ≥20 years.[2] Mitsuhashi *et al.* observed that the prevalence of overweight was 3.12% among children aged 6 years in 1985, and it steadily increased to 4.68% in 2005.[3]

A particular form of kidney disease, so-called obesity-related glomerulopathy (ORG), is characterized by glomerulomegaly with or without focal segmental glomerulosclerosis (FSGS), and the incidence of ORG has increased during the last decade with

Correspondence: Yukihiko Kawasaki, MD PhD, Department of Pediatrics, Fukushima Medical University School of Medicine, 1 Hikarigaoka, Fukushima City, Fukushima 960-1295, Japan. Email: kyuki@fmu.ac.jp

Received 4 March 2013; revised 19 May 2013; accepted 23 August 2013.
doi: 10.1111/ped.12213

Pituitary
DOI 10.1007/s11102-013-0546-5

A novel mutation in *SOX3* polyalanine tract: a case of kabuki syndrome with combined pituitary hormone deficiency harboring double mutations in *MLL2* and *SOX3*

Masaki Takagi · Tomohiro Ishii · Chiharu Torii · Kenjiro Kosaki · Tomonobu Hasegawa

Abstract
Introduction Both duplications encompassing *SOX3* and loss-of function mutations in *SOX3* have been reported in a minor portion of X-linked isolated growth hormone deficiency (GHD) or combined pituitary hormone deficiency (CPHD) patients with or without mental retardation.
Patients and methods We report a Japanese male patient with molecularly confirmed Kabuki syndrome who was found to have CPHD. We analyzed all coding exons and flanking introns of currently known nine genes responsible for CPHD by PCR-based sequencing.
Results In this CPHD patient, we identified a novel hemizygous 21-base pair deletion, resulting in the loss of 7 alanine residues from polyalanine (PA) tracts of *SOX3*. The clinically and endocrinologically normal mother of the patient carried the same deletion in a heterozygous manner. In vitro experiments showed that the del 7A SOX3 had increased transactivation of the *HESX1* promoter.
Conclusion Our study provides additional evidence that deletion in PA tracts of *SOX3* is associated with hypopituitarism. Female carriers of *SOX3* PA tract deletions will show a broad phenotypic spectrum, ranging from clinically normal to CPHD.

M. Takagi · T. Ishii · T. Hasegawa (✉)
Department of Pediatrics, Keio University School of Medicine, 35 Shinanomachi, Shinjuku-ku, Tokyo 160-8582, Japan
e-mail: thaseg@a6.keio.jp

M. Takagi
Department of Endocrinology and Metabolism, Tokyo Metropolitan Children's Medical Center, Tokyo, Japan

C. Torii · K. Kosaki
Center for Medical Genetics, Keio University School of Medicine, Tokyo, Japan

Published online: 18 December 2013

Keywords CPHD · SOX3 · PA tract

Introduction

SOX3 (OMIM#313430) is a member of the SOX (SRY related high mobility group box) family of transcription factors, expressed in neuroepithelial progenitor and stem cells from the earliest stages of development and its dosage is critical for normal pituitary development [1]. SOX3 contains a high mobility group DNA-binding domain, and 4 polyalanine (PA) tracts shown to be involved in transcriptional activation. Both duplications encompassing *SOX3* and loss-of function mutations in *SOX3* have been reported in a minor portion of X-linked isolated growth hormone deficiency (GHD) or combined pituitary hormone deficiency (CPHD) patients with or without mental retardation [2–5]. Here, we report the case of a Japanese patient with Kabuki syndrome (OMIM#147920, KS), who exhibited CPHD, harboring double mutations in *MLL2* and *SOX3*.

KS is a multiple congenital anomaly/intellectual disability syndrome characterized by a distinct dysmorphic facial appearance [6, 7]. Recently, mutations in *MLL2* gene (OMIM# 602113), encoding an H3K4 histone methyl transferase, which acts as an epigenetic transcriptional activator during growth and development, have been reported to be the cause of KS [8]. Endocrinological abnormalities, except for premature thelarche, are rare (or not well described) in KS. To date, GHD has been identified in very few cases [9–14]. To the best of our knowledge, no CPHD has been reported in a KS case. The lack of previous reports on this specific combination of relatively rare conditions led us to perform a genetic screen of 9 currently known CPHD-associated genes, and we identified a novel hemizygous 21-base pair deletion resulting in the

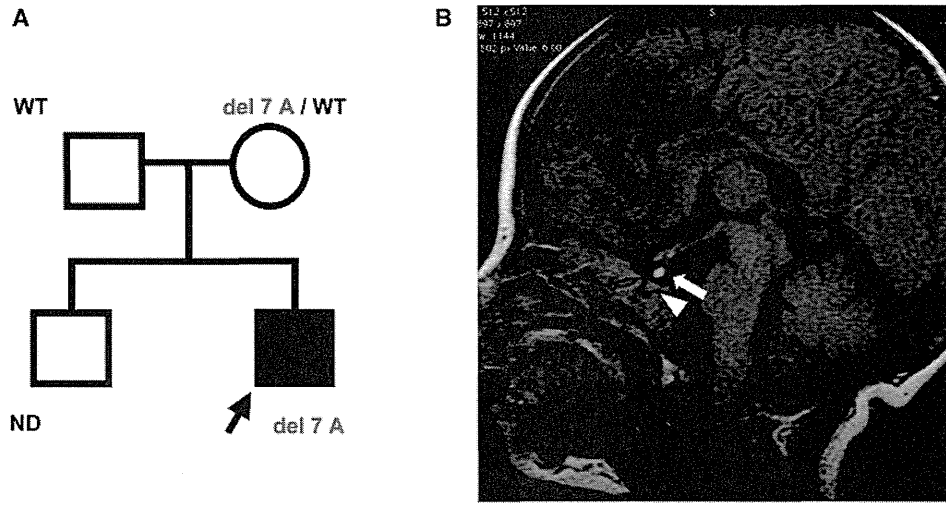

Fig. 1 Features of the propositus. **a** The pedigrees of the family. The *arrow* indicates the propositus. **b** Brain magnetic resonance imaging (*MRI*) at the age of 3 months. An ectopic posterior gland (*arrow*) and a small anterior pituitary (*arrowhead*) are shown

loss of 7 alanine residues between codons 239 and 245 (p.Ala239_245 del 7 A) from the first PA tract of *SOX3*. Our study provides additional evidence that deletion in the first PA tract of SOX3 is associated with hypopituitarism.

Materials and methods

Patient report

The propositus was a 5-year-old Japanese boy born at 37 weeks of gestation after an uncomplicated pregnancy and delivery. The parents were nonconsanguineous and phenotypically normal. He had 1 older brother, who had no relevant clinical problems (Fig. 1a). His birth weight was 2,738 g (−0.7 SD), and the length was 45.0 cm (−1.9 SD). The Apgar scores were 6 and 7 at 1 and 5 min, respectively. At birth, several dysmorphic features including eversion of the lower lateral eyelid, arched eyebrows with the lateral one-third sparse, depressed nasal tip, and prominent ears were observed. At 1 week of age, he was diagnosed with congenital heart disease, including a ventriculoseptal defect, an atrial septal defect, and mitral stenosis. He exhibited postnatal growth retardation and a developmental delay. He could not sit unassisted until the age of 23 months. Severe mental retardation, with a developmental quotient (DQ) of 49, was noted at the age of 2 years. An ABR examination revealed a hearing loss: 60 dB on the right side and 50 dB on the left side at the age of 2 years. A skeletal survey revealed sagittal cleft of vertebral body. His G-banded karyotype was normal. He was diagnosed with KS.

As a neonate, he was diagnosed with central hypothyroidism on the basis of a low free T4 (0.52 ng/dL: Ref. 0.99–1.91) with an inadequately increased TSH level of 6.27 mU/L (Ref. 0.77–7.3). There was no micropenis or undescended testes. Prolonged cholestasis and frequent episodes of hypoglycemia were noted at the age of 2 months. He was diagnosed with cortisol deficiency on the basis of low cortisol (10.9 μg/dL) at the time of severe hypoglycemia (glucose 0.9 mmol/L). Brain magnetic resonance imaging (MRI) at the age of 3 months showed a small anterior pituitary with a visible stalk, and an ectopic posterior pituitary gland (EPP) (Fig. 1b). As an extra pituitary finding, a hypoplastic corpus callosum was noted. Replacement therapy with l-thyroxine and hydrocortisone was started at 1 and 7 months of age, respectively. At the age of 2 years, his height and weight were 72.0 cm (−5.1 SD) and 8.0 kg (−3.3 SD) respectively. He presented with persistent hypoglycemia, low serum concentrations of IGF-I, and impaired GH response on arginine hydrochloride testing (peak GH 3.2 ng/mL, Ref. >6.0), and replacement therapy with recombinant human GH was started. After starting GH therapy, hypoglycemia has not been recorded. Follow-up MRI at the age of 2 years showed anterior pituitary hypoplasia, poorly developed sella turcica, a visible, but thin stalk, and EPP. Basal prolactin concentration was 6.9 and 3.9 ng/mL at the ages of 1, 2 years respectively.

Mutation analysis of *MLL2* gene and the genes responsible for CPHD

After genetic counseling, we obtained written informed consent from the patient or parents for molecular studies, which were approved by the Institutional Review Board of the Keio University School of Medicine. Genomic DNAs were extracted from peripheral blood of the patients and parents by using standard techniques. We analyzed all the coding exons and flanking introns of *MLL2*. For genetic screening of CPHD, we analyzed all coding exons and flanking introns of *POU1F1, PROP1, HESX1, LHX3, LHX4, OTX2, SOX2, GLI2,* and *SOX3* by PCR-based sequencing. We screened for deletion/duplication involving

POU1F1, PROP1, HESX1, LHX3, and *LHX4* by MLPA analyses (SALSA MLPA KIT P216; MRC-Holland, Amsterdam, The Netherlands). We tested detected sequence variation against 100 (male 65, female 35) Japanese control subjects.

X-inactivation studies

The X-chromosome inactivation pattern of the unaffected mother was determined using the androgen receptor (*AR*) gene methylation assay [15]. In brief, leukocyte genomic DNA was PCR amplified with a fluorescent labeled forward primer and an unlabeled reverse primer flanking the CAG repeat region and the two methylation sensitive *Hpa*II sites at exon 1 of *AR*, before and after *Hpa*II digestion. PCR products were obtained from both active and inactive X chromosomes before *Hpa*II digestion and from inactive X chromosomes alone after *Hpa*II digestion. For the X-inactivation analysis, the PCR products obtained before and after *Hpa*II digestion were determined for size and examined for area under curve (AUC) on an ABI PRISM 3100 autosequencer using GeneScan (Applied Biosystems, Norwalk, CT). The X inactivation ratio was calculated using the area under curve.

Functional studies

To generate SOX3 expression vectors, the *SOX3* coding region was amplified from patients' and control DNA and cloned into pCMV-myc (Clontech, Palo Alto, CA). A luciferase reporter vector was constructed by inserting the *HESX1* promoter sequence (−405 to +267 bp) into a pGL4.24 [luc2P/minP] vector (Promega, Madison, WI). A transactivation assay was performed in COS1 cells using a dual-luciferase reporter assay system (Promega). For subcellular localization analyses, COS1 cells transfected with the myc-tagged SOX3 were fixed in 4 % paraformaldehyde, permeabilized with 0.2 % TritonX-100 and blocked in 10 % BSA in PBS. Cells were then incubated with a mouse anti-myc monoclonal antibody (Invitrogen) for 1 h. After washing, cells were incubated with 1:1,000 Alexa Fluor secondary antibodies (Cell Signaling Technology) in blocking buffer for 1 h. Cells were imaged using an IX-71 fluorescence microscope (Olympus, Tokyo, Japan). For immunoblot assays, COS1 cells transfected with the myc-tagged SOX3 were harvested, and nuclear protein was isolated with the NE-PER nuclear extraction reagent kit (Pierce, Rockford, IL). Western blotting was performed with a mouse anti-myc monoclonal antibody (Invitrogen).

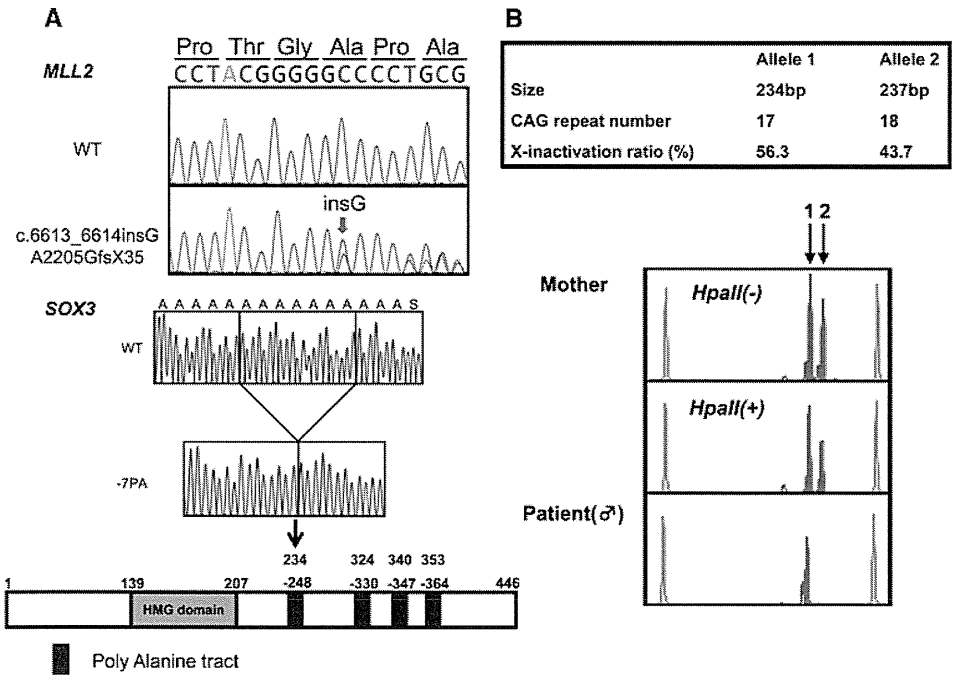

Fig. 2 Identification of mutations in *MLL2* and *SOX3*. **a** The *red arrow* indicates the mutation in *MLL2*. **b** We identified a hemizygous novel 21-base pair in-frame deletion, resulting in the loss of seven alanine residues between codons 239 and 245 (p.Ala239_245 del7A) of *SOX3*. **c** CAG repeat length and X-inactivation analyses. Before *Hpa*II digestion, two alleles have been delineated on the autosequencer. Allele 1, which represents mutated allele, is 234 bp long and contains 17 CAG repeats, and allele 2 is 237 bp long and contains 18 CAG repeats. The X-inactivation ratio is calculated using the AUCs before and after *Hpa*II digestion. In the mother, allele 1 is preferentially inactivated compared with allele 2 (Allele 1: 56.3 %, Allele 2: 43.7 %)

The sequences of the biotin-labeled double stranded oligonucleotide used as probe in the EMSA experiment was 5′-CAAACAAATAAACAATTAACTC-3′ [3]. Five microgram of nuclear protein extraction was incubated at room temperature in 20-μL binding reaction mixture contained 20 fmol probe, 50 mM KCl, 5 mM $MgCl_2$, 2.5 % glycerol, 0.05 % NP-40, and 1 μg poly (dI–dC) for 20 min. For competition experiments, a large excess (200×) of unlabeled competitor oligonucleotides was included in the binding reactions. The protein-DNA complexes were subject to gel electrophoresis and transferred to a nylon membrane. The biotin-labeled probe was detected with the Lightshift chemiluminescent EMSA kit (Pierce).

Results

Mutation analysis of *MLL2* gene and the genes responsible for CPHD

We identified a novel heterozygous frameshift mutation in *MLL2*, namely c.6613_6614insG, p.Ala2205GlyfsX38 (Fig. 2a). Familial gene analysis revealed that this mutation was de novo.

We also identified a hemizygous novel 21-base pair in-frame deletion, resulting in the loss of seven alanine residues between codons 239 and 245 (p.Ala239_245 del7A) of *SOX3* (Fig. 2b). This mutation was not detected in any of the 100 healthy controls and was absent from database, including dbSNP, the 1,000 Genomes Project, and Exome Variant Server, NHLBI Exome Sequencing Project. We detected no gross or exon-level deletions/duplications by the MLPA analyses. Genetic analyses showed that the clinically normal mother, whose adult height was 155.0 cm (−0.58 SD), carried the same 21-base pair deletion in a heterozygous manner and that the father did not. Baseline hormonal data (Table 1) and MRI findings of the mother were normal. No other family member was available for genetic studies.

Table 1 Endocrinological findings (baseline) in the mother

	Mother	Reference (adult)
GH (ng/mL)	0.2	0–23
IGF-1 (ng/mL)	135.0	Female: 73–542
TSH (μU/mL)	1.62	0.3–3.50
Free T4 (ng/dL)	1.2	1.09–2.55
Free T3 (pg/mL)	2.6	3.23–5.11
LH (mIU/mL)	7.8	Female: 1.4–15[a]
FSH (mIU/mL)	24.0	Female: 3–10[a]
PRL (ng/mL)	8.8	Female: 1.4–14.6
ACTH (pg/mL)	15.0	7.2–63.3
Cortisol (μg/dL)	11.6	7.6–21.4
Estradiol (pg/mL)	20	Female: 11–230[a]

[a] Follicular phase

X-inactivation studies

Preferential inactivation of the abnormal X-chromosome was shown (Fig. 2c).

Functional studies

In COS1 cells, WT SOX3 stimulated transcription of the *HESX1* reporter. The del 7 PA SOX3 mutant proteins had increased transactivation compared with WT SOX3 (Fig. 3a). Subcellular localization and western blotting

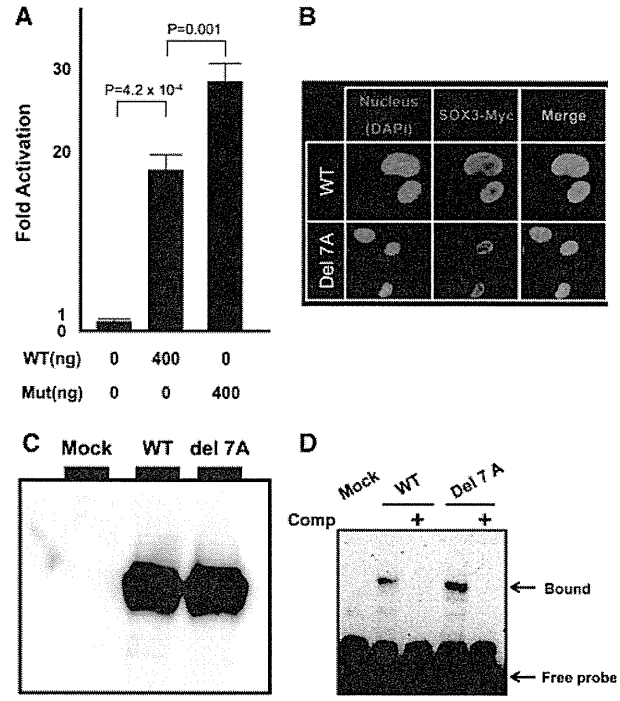

Fig. 3 Functional characterization of del 7 A SOX3. **a** Transactivation assays of del 7 A SOX3 using *HESX1* reporter COS1 cells were cotransfected with the pRL-CMV internal control vector, indicated amount (nanograms) of the effector plasmids, and the *HESX1* reporter. WT SOX3 stimulated transcription of the *HESX1* reporter. The del 7 PA SOX3 resulted in an approximately 1.5-fold increase in transcriptional activation compared with WT SOX3 ($p = 0.001$). The data are mean ± SEM of at least three independent experiments performed in triplicate transfections. **b** Subcellular localization analysis. We visualized and photographed COS1 cells transfected with myc-tagged SOX3 using an IX-71 fluorescence microscope, after mounting the cells in Vectashield-DAPI solution. The WT and del 7 A SOX3 are localized to the nucleus. **c** Western blot analysis showed that the expression of del 7 A SOX3 was comparable to that of the WT. **d** EMSA experiments WT SOX3 showed specific binding to the elements, which was competed by excess amount of (200 times) cold competitors. The del 7 A SOX3 bound with similar or slightly high efficiency to the WT SOX3

Table 2 Summary of the clinical phenotypes and MRI findings of *SOX3* mutations

Case	Age at evaluation	Sex	Clinical findings	Affected pituitary hormones	MRI findings	SOX3 mutation	Ref
I-1	3.0 (years)	Male	Short stature (−3.0 SD) Normal intelligence	GH	NA	+7 PA	5
I-2	1.5 (years)	Male	Short stature (−2.7 SD) Learning difficulties	GH	APH EPP		
II-1	9 (years)	Male	Short stature (−2.8 SD) Normal intelligence	GH	Normal AP EPP	+7 PA	4
II-2	12 (months)	Male	Normal intelligence	GH	APH EPP		
III-1	3.0 (years)	Male	Short stature (−2.5 SD) Normal intelligence	GH, TSH, LH/FSH, ACTH	NA	+7 PA	3
III-2	4.5 (years)	Male	Short stature (−2.5 SD) Normal intelligence	GH, TSH, LH/FSH, ACTH	APH EPP		
III-3	2.7 (years)	Male	Short stature (−1.3 SD)	GH, TSH, LH/FSH, ACTH	APH EPP		
IV		Male	Short stature Mental retardation	GH	NA	+11 PA	2
V		Male	Short stature Mental retardation	No pituitary phenotype	NA	del 9 PA	2
VI	7.5 (years)	Female	Short stature (−3.1 SD) Normal intelligence	GH, TSH, LH/FSH	Enlarged AP NPP	del 6 PA	5
Our case	5.0 (years)	Male	Short stature Mental retardation	GH, TSH, ACTH	APH EPP	del 7 PA	

AP anterior pituitary, *APH* anterior pituitary hypoplasia, *EPP* ectopic posterior pituitary, *NPP* normal posterior pituitary, *NA* not available

revealed no significant difference between WT and mutant SOX3 (Fig. 3b, c), indicating that protein expression and nuclear targeting were not affected by the mutation. WT SOX3 showed specific binding to the elements, which was competed by excess amount of (200 times) cold competitors. The del 7 A SOX3 bound with similar or slightly high efficiency to the WT SOX3 (Fig. 3d).

Discussion

To date, 4 intragenic mutations in *SOX3* have been reported and all of them involve expansions or deletions of the first PA tract [2–5]. Here, we summarize the clinical phenotypes and MRI findings of *SOX3* mutations reported thus far (Table 2). At least 3 pedigrees harboring 7 alanine expansions (+7 PA) have been reported and their clinical phenotype or MRI findings have been shown to be variable among patients with the same *SOX3* mutation. In contrast to PA expansions, deletions are even rarer. A 9-alanine deletion (del 9 PA) in 2 brothers with mental retardation, but without a clearly defined pituitary phenotype and a 6-alanine deletion (del 6 PA) in a female patient with CPHD have been reported. Our case is the third report of a PA tract deletion, which had increased transactivation of SOX3 target genes as previously described by Alatzoglou et al. [5]. We believe that our observation will provide additional evidence that deletion in the PA tracts of *SOX3* is associated with hypopituitarism and will provide clinical information to extend the phenotypic spectrum of patients with PA tract deletion of *SOX3*.

A female patient with a heterozygous del 6 PA exhibited CPHD, without skewed X inactivation in the genomic DNA extracted from her peripheral blood [5]. On the other hand, the mother of our patient, carrying a del 7 PA in a heterozygous manner, was clinically and endocrinologically normal, which may be partially due to skewed X-inactivation. This indicates that female carriers of *SOX3* PA tract deletion mutations will show a broad phenotypic spectrum, from clinically normal to CPHD.

Approximately 55–80 % of KS patients are estimated to have mutations in the *MLL2* gene, encoding a large 5,537-residue protein including 7 PHD fingers, FYRN, FYRC, and a SET domain [8, 16–19]. The SET domain of MLL2 confers strong histone 3 lysine 4 methyltransferase activity and is important in the epigenetic control of active chromatin states [20]. The c.6613_6614insG mutation in *MLL2* results in a premature termination codon (PTC) with mRNA that is predicted to be destroyed by the process of nonsense-mediated RNA decay. If translated, this abnormal

transcript would generate a protein lacking one of the 7 PHD fingers, the entire of the FYRN, FYRC, and SET domain. Additionally, the de novo *MLL2* mutation of our patient indicates that the occurrence of KS and *SOX3* associated CPHD is a coincidence.

In summary, we report the case of a KS patient with CPHD, carrying mutations in *MLL2* and *SOX3*. Our study provides additional evidence that deletion in the PA tracts of *SOX3* is associated with hypopituitarism.

Acknowledgments We thank the patient and his family for participation in this study. We thank Kazue Kinoshita for technical assistance. This work was supported by a Grant-in-Aid for the Health Science Research Grant for Research on Applying Health Technology [Jitsuyoka (Nanbyo)-Ippan-014 (23300102)] from the Ministry of Health, Labour and Welfare of Japan.

Conflict of interest The authors have declared no conflicts of interest.

References

1. Collignon J, Sockanathan S, Hacker A, Cohen-Tannoudji M, Norris D, Rastan S, Stevanovic M, Goodfellow PN, Lovell-Badge R (1996) A comparison of the properties of SOX-3 with Sry and two related genes, Sox-1 and Sox-2. Development 122(2):509–520
2. Laumonnier F, Ronce N, Hamel BC, Thomas P, Lespinasse J, Raynaud M, Paringaux C, Van Bokhoven H, Kalscheuer V, Fryns JP, Chelly J, Moraine C, Briault S (2002) Transcription factor SOX3 is involved in X-linked mental retardation with growth hormone deficiency. Am J Hum Genet 71(6):1450–1455
3. Woods KS, Cundall M, Turton J, Rizotti K, Mehta A, Palmer R, Wong J, Chong WK, Al-Zyoud M, El-Ali M, Otonkoski T, Martinez-Barbera JP, Thomas PQ, Robinson IC, Lovell-Badge R, Woodward KJ, Dattani MT (2005) Over- and underdosage of SOX3 is associated with infundibular hypoplasia and hypopituitarism. Am J Hum Genet 76(5):833–849
4. Burkitt Wright EM, Perveen R, Clayton PE, Hall CM, Costa T, Procter AM, Giblin CA, Donnai D, Black GC (2009) X-linked isolated growth hormone deficiency: expanding the phenotypic spectrum of *SOX3* polyalanine tract expansions. Clin Dysmorphol 18(4):218–221
5. Alatzoglou KS, Kelberman D, Cowell CT, Palmer R, Arnhold IJ, Melo ME, Schnabel D, Grueters A, Dattani MT (2011) Increased transactivation associated with *SOX3* polyalanine tract deletion in a patient with hypopituitarism. J Clin Endocrinol Metab 96(4): 685–690
6. Niikawa N, Matsuura N (1981) Kabuki make-up syndrome: a syndrome of mental retardation, unusual facies, large and protruding ears, and postnatal growth deficiency. J Pediatr 99(4): 565–569
7. Kuroki Y, Suzuki Y, Chyo H, Hata A, Matsui I (1981) A new malformation syndrome of long palpebral fissures, large ears, depressed nasal tip, and skeletal anomalies associated with postnatal dwarfism and mental retardation. J Pediatr 99(4):570–573
8. Ng SB, Bigham AW, Buckingham KJ, Hannibal MC, McMillin MJ, Gildersleeve HI, Beck AE, Tabor HK, Cooper GM, Mefford HC, Lee C, Turner EH, Smith JD, Rieder MJ, Yoshiura K, Matsumoto N, Ohta T, Niikawa N, Nickerson DA, Bamshad MJ, Shendure J (2010) Exome sequencing identifies *MLL2* mutations as a cause of Kabuki syndrome. Nat Genet 42(9):790–793
9. Niikawa N, Kuroki Y, Kajii T, Matsuura N, Ishikiriyama S, Tonoki H, Ishikawa N, Yamada Y, Fujita M, Umemoto H (1988) Kabuki make-up (Niikawa-Kuroki) syndrome: a study of 62 patients. Am J Med Genet 31(3):565–589
10. Handa Y, Maeda K, Toida M, Kitajima T, Ishimaru J, Nagai A, Oka N (1991) Kabuki make-up syndrome (Niikawa-Kuroki syndrome) with cleft lip and palate. J Craniomaxillofac Surg 19(3):99–101
11. Satoh M, Arakawa K, Yokoya S, Morooka K (1993) A case of Kabuki make-up syndrome associated with growth hormone deficiency. Clin Pediatr Endocrinol 2(1):13–16
12. Tawa R, Kaino Y, Ito T, Goto Y, Kida K, Matsuda H (1994) A case of Kabuki make-up syndrome with central diabetes insipidus and growth hormone neurosecretory dysfunction. Acta Paediatr Jpn 36(4):412–415
13. Devriendt K, Lemli L, Craen M, de Zegher F (1995) Growth hormone deficiency and premature thelarche in a female infant with kabuki makeup syndrome. Horm Res 43(6):303–306
14. Gabrielli O, Bruni S, Bruschi B, Carloni I, Coppa GV (2002) Kabuki syndrome and growth hormone deficiency: description of a case treated by long-term hormone replacement. Clin Dysmorphol 11(1):71–72
15. Allen RC, Zoghbi HY, Moseley AB, Rosenblatt HM, Belmont JW (1992) Methylation of HpaII and HhaI sites near the polymorphic CAG repeat in the human androgen-receptor gene correlates with X chromosome inactivation. Am J Hum Genet 51(6):1229–1239
16. Micale L, Augello B, Fusco C, Selicorni A, Loviglio MN, Silengo MC, Reymond A, Gumiero B, Zucchetti F, D'Addetta EV, Belligni E, Calcagnì A, Digilio MC, Dallapiccola B, Faravelli F, Forzano F, Accadia M, Bonfante A, Clementi M, Daolio C, Douzgou S, Ferrari P, Fischetto R, Garavelli L, Lapi E, Mattina T, Melis D, Patricelli MG, Priolo M, Prontera P, Renieri A, Mencarelli MA, Scarano G, della Monica M, Toschi B, Turolla L, Vancini A, Zatterale A, Gabrielli O, Zelante L, Merla G (2011) Mutation spectrum of MLL2 in a cohort of Kabuki syndrome patients. Orphanet J Rare Dis. 9(6):38–45
17. Hannibal MC, Buckingham KJ, Ng SB, Ming JE, Beck AE, McMillin MJ, Gildersleeve HI, Bigham AW, Tabor HK, Mefford HC, Cook J, Yoshiura K, Matsumoto T, Matsumoto N, Miyake N, Tonoki H, Naritomi K, Kaname T, Nagai T, Ohashi H, Kurosawa K, Hou JW, Ohta T, Liang D, Sudo A, Morris CA, Banka S, Black GC, Clayton-Smith J, Nickerson DA, Zackai EH, Shaikh TH, Donnai D, Niikawa N, Shendure J, Bamshad MJ (2011) Spectrum of MLL2 (ALR) mutations in 110 cases of Kabuki syndrome. Am J Med Genet A 155A(7):1511–1516
18. Paulussen AD, Stegmann AP, Blok MJ, Tserpelis D, Posma-Velter C, Detisch Y, Smeets EE, Wagemans A, Schrander JJ, van den Boogaard MJ, van der Smagt J, van Haeringen A, Stolte-Dijkstra I, Kerstjens-Frederikse WS, Mancini GM, Wessels MW, Hennekam RC, Vreeburg M, Geraedts J, de Ravel T, Fryns JP, Smeets HJ, Devriendt K, Schrander-Stumpel CT (2011) MLL2 mutation spectrum in 45 patients with Kabuki syndrome. Hum Mutat 32(2):2018–2025
19. Li Y, Bögershausen N, Alanay Y, Simsek Kiper PO, Plume N, Keupp K, Pohl E, Pawlik B, Rachwalski M, Milz E, Thoenes M, Albrecht B, Prott EC, Lehmkühler M, Demuth S, Utine GE, Boduroglu K, Frankenbusch K, Borck G, Gillessen-Kaesbach G, Yigit G, Wieczorek D, Wollnik B (2011) A mutation screen in patients with Kabuki syndrome. Hum Genet 136(6):715–724
20. Issaeva I, Zonis Y, Rozovskaia T, Orlovsky K, Croce CM, Nakamura T, Mazo A, Eisenbach L, Canaani E (2007) Knockdown of ALR (MLL2) reveals ALR target genes and leads to alterations in cell adhesion and growth. Mol Cell Biol 27(5):1889–1903

European Journal of Medical Genetics 56 (2013) 526–528

Contents lists available at ScienceDirect

European Journal of Medical Genetics

journal homepage: http://www.elsevier.com/locate/ejmg

Array report

A 2.0 Mb microdeletion in proximal chromosome 14q12, involving regulatory elements of *FOXG1*, with the coding region of *FOXG1* being unaffected, results in severe developmental delay, microcephaly, and hypoplasia of the corpus callosum

Masaki Takagi [a,b], Goro Sasaki [c], Toshikatsu Mitsui [a], Misa Honda [c], Yoko Tanaka [c], Tomonobu Hasegawa [a,*]

[a] *Department of Pediatrics, Keio University School of Medicine, Tokyo, Japan*
[b] *Department of Endocrinology and Metabolism, Tokyo Metropolitan Children's Medical Center, Tokyo, Japan*
[c] *Department of Pediatrics, Tokyo Dental College Ichikawa General Hospital, Ichikawa, Japan*

ARTICLE INFO

Article history:
Received 30 August 2012
Accepted 30 May 2013
Available online 26 July 2013

Keywords:
FOXG1
PRKD1
Regulatory elements
14q12
Array CGH assay

ABSTRACT

We identified 2.0 Mb of a novel deletion on chromosome 14q12, involving 8 genes and putative regulatory elements of *FOXG1* by array CGH in a patient with severe growth and psychomotor retardation, hypotonia, microcephaly, dysmorphic face, and hypoplasia of the corpus callosum. Case of a submicroscopic 14q12 deletion, involving regulatory elements of *FOXG1*, with the coding region of *FOXG1* being unaffected, is extremely rare.

Using fibroblast cell line established from the patient, we showed that the expression level of *FOXG1* in our patient was decreased. Our finding provides additional evidence that not only over-dosage of FOXG1 as previously mentioned, under-dosage of FOXG1 is also associated with phenotype, overlapping between congenital variant of Rett syndrome with *FOXG1* mutations and 14q12 microdeletion, not including the coding region of *FOXG1*. Though the gene dosage of *FOXG1* appears to be critical for the normal development of brain, the complex mechanism of its regulation of gene expression remains to be elucidated.

1. Methods of detection

1.1. Array CGH analysis

After genetic counseling, we obtained written informed consent from the parents for molecular studies, which were approved from the Institutional Review Board of the Keio University School of Medicine. Genomic DNAs were extracted from peripheral blood of the patient and parents using standard techniques, subjected to array comparative genomic hybridization (aCGH) with the Agilent 4 × 180K SurePrint G3 Human CGH Microarray (catalog no. G4449A; Agilent Technologies, Santa Clara, CA).

1.2. Chromosomal anomaly

The array CGH assay for the patient revealed a heterozygous interstitial deletion, which was of estimated minimum extent 2.05 Mb, extending from bp 29,677,089 to bp 31,731,999 on chromosome 14q12 (NCBI Build 37/hg 19) (Fig. 1A). Maximum size was 2.14 Mb, from bp 29,615,149 to bp 31,755,257. The deletion included 8 genes (*PRKD1*, *G2E3*, *SCFD1*, *COCH*, *STRN3*, *MIR624*, *AP4S1*, and *HECTD1*).

1.3. Method of confirmation

FISH was performed on metaphase slides from peripheral blood lymphocytes using standard techniques. The deletion was confirmed using the RP11-369O9 clones (Fig. 1B). CGH analysis of the parents revealed that this deletion was *de novo* (data not shown).

* Corresponding author. Department of Pediatrics, Keio University School of Medicine, 35 Shinanomachi, Shinjuku-ku, Tokyo 160-8582, Japan. Tel.: +81 3 3353 1211.
E-mail address: thaseg@a6.keio.jp (T. Hasegawa).

1769-7212/$ – see front matter © 2013 Elsevier Masson SAS. All rights reserved.
http://dx.doi.org/10.1016/j.ejmg.2013.05.012

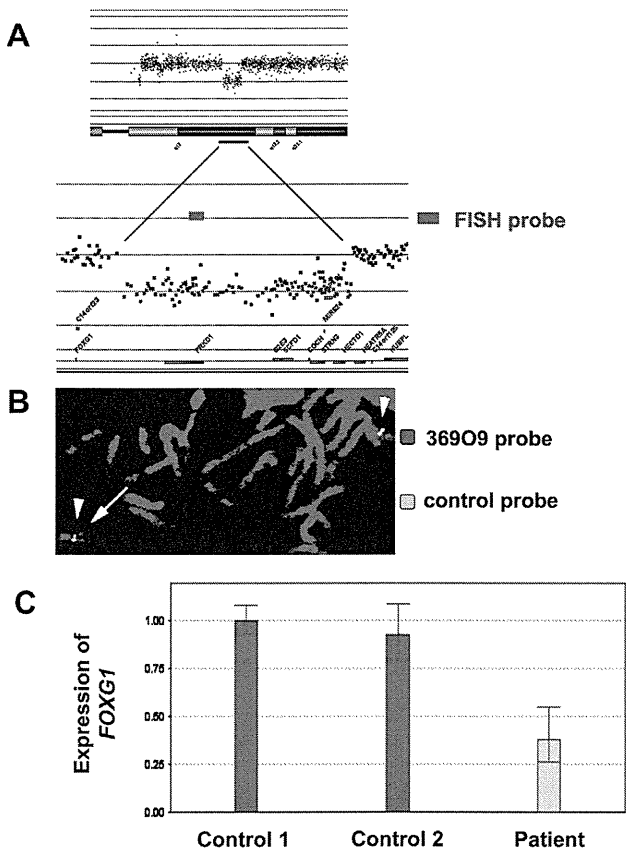

Fig. 1. Result of CGH array analysis, FISH validation, and quantification of the expression of *FOXG1*. A: Graphical representation of the results of the array CGH analysis [Agilent 4 × 180K SurePrint G3 Human CGH Microarray] shows a 2.0 Mb interstitial deletion of 14q12, including 8 genes. B: FISH analysis for validation of array CGH result. The patient under study shows a deletion of RP11-369O9 [red] located on 14q12 (arrow). C: Real-Time PCR revealed that the level of *FOXG1* transcripts of the patient was about 40% the control level.

1.4. Expression of FOXG1 in the patient with 14q12 microdeletion

Total RNA was extracted from lymphoblastoid cell line established from the patient and cDNA synthesis was performed with the SuperScript III reverse transcriptase kit (Invitrogen, Carlsbad, CA) with oligoDT primers. Real-time quantitative PCR was performed on the ABI PRISM 7500 Fast Real-Time PCR System (Applied Biosystems, Foster City, CA). For PCR reaction, we used SYBR Premix Ex Taq II (Takara, Otsu, Japan). The relative quantification was performed with the 2-DDCt method relative to a constitutively expressed gene (*GAPDH*). All reactions were carried out in triplicate and expression levels were determined in 3 independent experiments. Real-Time PCR revealed that the level of *FOXG1* transcripts of the patient was about 40% the control level (Fig. 1C).

2. Clinical description

The patient, an 11-year-old Japanese boy, was the first child of non-consanguineous healthy parents. He was born at term after uneventful pregnancy and delivery, and his birth weight, length, and OFC were 2706 g (10–25th percentile), 49.0 cm (25–50th percentile), and 31.5 cm (3rd–10th percentile), respectively. At the age of 6 month, he was referred to our hospital for evaluation of developmental delay and dysmorphic features. He exhibited hypotonia with incomplete head control, microcephaly (OFC, 40.1 cm, below 3rd percentile), and facial anomaly including hypertelorism, epicanthal folds, depressed and broad nasal bridge, and short neck (Fig. 2A). Cortical atrophy of parietooccipital lobes, delayed myelination, and hypoplasia of the corpus callosum (HCC) were demonstrated on brain MRI (Fig. 2B), while no malformation was displayed in heart and kidney ultrasonography, and no overt hearing loss was evidenced in auditory brainstem response. He also presented frequent generalized seizures, which were well controlled with phenobarbital and sodium valproate. Growth and psychomotor development were severely retarded. At 11 years of age, his weight, length, and OFC were 15.5 kg (below 3 percentile), 107.0 cm (below 3 percentile), and 47.4 cm (below 3rd percentile), respectively. No apparent skeletal deformity was documented on X-ray, and plasma concentrations of thyroxine and insulin-like growth factor-1 were within normal ranges. Due to severe psychomotor retardation, he remains wheelchair-bound and nonverbal.

3. Discussion

We identified 2.0 Mb of a novel deletion on chromosome 14q12, involving 8 genes and putative regulatory elements of *FOXG1* by using array CGH in a patient with severe growth and psychomotor

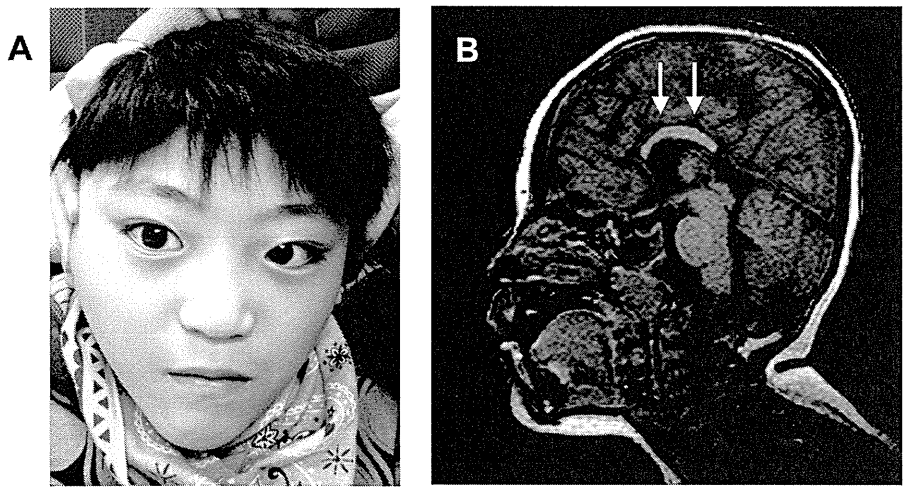

Fig. 2. Features of the patient with deletion on chromosome 14q12. A: Photographs of the patient at 10 years of age. Facial features demonstrated ocular hypertelorism, epicanthal folds, depressed and broad nasal bridge, and short neck. B: Brain imaging in the patient at the age of 5 years. Arrow indicates hypoplasia of the corpus callosum.

retardation, hypotonia, acquired microcephaly, dysmorphic face, and HCC. *FOXG1* encodes forkhead box protein G1, which plays important roles in the establishment of the regional subdivision of the developing brain and development of the telencephalon, and its defect causes a congenital variant of Rett syndrome (RTTCV, MIM #613454) [1]. RTTCV is characterized by severe neurodevelopmental impairments including psychomotor regression, hypotonia, progressive microcephaly, and HCC, which are comparable to the manifestations of our patient.

Case of a submicroscopic 14q12 deletion, involving regulatory elements of *FOXG1*, with the coding region of *FOXG1* being unaffected, is extremely rare. In addition to a patient reported by Kortum et al. [2], a recently published paper by Allou et al. [3] reported three 14q12 deletions that do not include the *FOXG1* coding region and were associated with phenotypes similar to patients with *FOXG1* mutations. Allou et al. mapped a putative long-range *FOXG1* regulatory element in a 0.43 Mb DNA segment encompassing the *PRKD1* locus. Using fibroblast cells established from these three patients, with increased expression level of *FOXG1*, they also showed that a cis-acting regulatory sequence, acting as a silencer, was located more than 0.6 Mb away from *FOXG1* (Fig. 3). Subsequently, Ellaway et al. reported three additional patients with severe intellectual impairment, early-onset developmental delay, postnatal microcephaly, and hypotonia, harboring 14q12 deletions that do not include the *FOXG1* coding region [4]. As is in our case, expression level of *FOXG1* in two of three patients report by Ellaway et al. was decreased. These finding strongly suggests that both over- and underdosage of FOXG1 are associated with similar phenotype, overlapping between RTTCV with *FOXG1* mutations and 14q12 microdeletion, not including the coding region of *FOXG1*. Interestingly, one patient with a 4.5 Mb duplication including *FOXG1* showed *FOXG1* downregulation [3,5]. This finding supports at the molecular level the phenotypic similarities between deletion and duplication cases.

Of the eight deleted genes in our case, whereas seven genes have been implicated in any known Copy Number Variations, the remaining gene *PRKD1* encodes a serine/threonine kinase that regulates a variety of cellular functions. In rodent model, PRKD1 are strongly expressed in the ventricular layer of the neocortex, striatum, septum, choroid plexus, and superior colliculus of mouse embryo [6], supporting developmental roles in central nervous system. Notably, all reported deletions distal to *FOXG1* also affect *PRKD1*. To determine whether a defect in the regulatory elements of *FOXG1* is sufficient for disease onset or whether *PRKD1* is responsible for a clinical condition overlapping the FOXG1/RTTCV, further studies or cases with intragenic mutations in *PRKD1* may be required. A number of CNVs in the general population are susceptibility alleles for common neuropsychiatric disorders, so some caution should be also paid to the 7 genes, which have been considered phenotypically neutral.

In summary, we identified 2.0 Mb of a novel deletion on chromosome 14q12, involving 8 genes and putative regulatory elements of *FOXG1* by array CGH in a patient with severe neurodevelopmental defects. Our finding provides additional evidence that not only over-dosage of FOXG1 as previously mentioned, under-dosage of FOXG1 is also associated with phenotype, overlapping between RTTCV with *FOXG1* mutations and 14q12 microdeletion, not including the coding region of *FOXG1*. Though the gene dosage of *FOXG1* appears to be critical for the normal development of brain, the complex mechanism of its regulation of gene expression remains to be elucidated. To correlate genotype to phenotype, clinical characterization of further deletion cases and saturation of the deletion map of this region is necessary to accomplish this task.

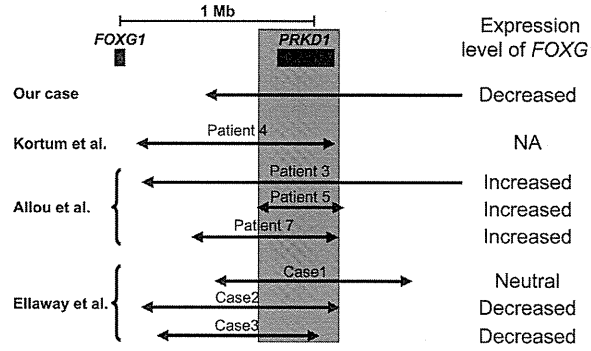

Fig. 3. Overview of the deletion in our patient and 7 previously reported deletions involving distal to *FOXG1*. Red shaded area indicates the putative long-range *FOXG1* regulatory element in a 0.43 Mb DNA segment encompassing the *PRKD1* locus mapped by Allou et al. Expression levels of *FOXG1* are listed on the right. NA, not analyzed.

Conflict of interest

The authors have nothing to declare.

Acknowledgments

We thank the patient and their families for participation in this study. We thank Kazue Kinoshita for technical assistance; Dr. Hirofumi Ohashi for establishing the Epstein–Barr virus transformed lymphocytes from the patient.

This work was supported by a Grant-in-Aid for the Health Science Research Grant for Research on Applying Health Technology [Jitsuyoka (Nanbyo)-Ippan-014 (23300102)] from the Ministry of Health, Labor and Welfare of Japan.

References

[1] F. Ariani, G. Hayek, D. Rondinella, R. Artuso, M.A. Mencarelli, A. Spanhol-Rosseto, M. Pollazzon, S. Buoni, O. Spiga, S. Ricciardi, I. Meloni, I. Longo, F. Mari, V. Broccoli, M. Zappella, A. Renieri, FOXG1 is responsible for the congenital variant of Rett syndrome, Am. J. Hum. Genet. 83 (2008) 89–93.

[2] F. Kortüm, S. Das, M. Flindt, D.J. Morris-Rosendahl, I. Stefanova, A. Goldstein, D. Horn, E. Klopocki, G. Kluger, P. Martin, A. Rauch, A. Roumer, S. Saitta, L.E. Walsh, D. Wieczorek, G. Uyanik, K. Kutsche, W.B. Dobyns, The core FOXG1 syndrome phenotype consists of postnatal microcephaly, severe mental retardation, absent language, dyskinesia, and corpus callosum hypogenesis, J. Med. Genet. 48 (2011) 396–406.

[3] L. Allou, L. Lambert, D. Amsallem, E. Bieth, P. Edery, A. Destrée, F. Rivier, D. Amor, E. Thompson, J. Nicholl, M. Harbord, C. Nemos, A. Saunier, A. Moustaïne, A. Vigouroux, P. Jonveaux, C. Philippe, 14q12 and severe Rett-like phenotypes: new clinical insights and physical mapping of FOXG1-regulatory elements, Eur. J. Hum. Genet. 20 (2012) 1216–1223.

[4] C.J. Ellaway, G. Ho, E. Bettella, A. Knapman, F. Collins, A. Hackett, F. McKenzie, A. Darmanian, G.B. Peters, K. Fagan, J. Christodoulou, 14q12 microdeletions excluding FOXG1 give rise to a congenital variant Rett syndrome-like phenotype, Eur. J. Hum. Genet. 12 (2012) 1–6.

[5] A. Yeung, D. Bruno, I.E. Scheffer, D. Carranza, T. Burgess, H.R. Slater, D.J. Amor, 4.45 Mb microduplication in chromosome band 14q12 including FOXG1 in a girl with refractory epilepsy and intellectual impairment, Eur. J. Med. Genet. 52 (2009) 440–442.

[6] H. Oster, D. Abraham, M. Leitges, Expression of the protein kinase D (PKD) family during mouse embryogenesis, Gene Expr. Patterns 6 (2006) 400–408.

RESEARCH LETTER

AMERICAN JOURNAL OF medical genetics PART A

A Recurrent Mutation in the 5′-UTR of *IFITM5* Causes Osteogenesis Imperfecta Type V

Masaki Takagi,[1,2] Shuhei Sato,[3] Keiichi Hara,[4] Chihiro Tani,[5] Osamu Miyazaki,[6] Gen Nishimura,[7] and Tomonobu Hasegawa[1]*

[1]Department of Pediatrics, Keio University School of Medicine, Tokyo, Japan

[2]Department of Endocrinology and Metabolism, Tokyo Metropolitan Children's Medical Center, Tokyo, Japan

[3]Perinatal Medical Center of Aomori Prefectural Central Hospital, Aomori, Japan

[4]Department of Pediatrics, Kure Medical Center, Hiroshima, Japan

[5]Department of Radiology, Hiroshima City Hospital, Hiroshima, Japan

[6]Department of Radiology, National Center for Child Health and Development, Tokyo, Japan

[7]Department of Radiology, Tokyo Metropolitan Children's Medical Center, Tokyo, Japan

Manuscript Received: 20 September 2012; Manuscript Accepted: 11 April 2013

TO THE EDITOR:

Osteogenesis imperfecta (OI) comprises a heterogeneous group of connective tissue disorders characterized by fragile bones with susceptibility to fractures. Recent investigations have revealed that OI is caused not only by mutations in collagen type I genes, but also in genes responsible for the post-translational processing of type I procollagen, which lead to the molecular-genetic division of OI into 11 types [Forlino et al., 2011]. Among them, type V OI (OI-V: OMIM #610967) is a variant of OI inherited as an autosomal dominant trait and has distinctive clinical and histologic manifestations [Glorieux et al., 2000]. Affected individuals develop ossifications of the interosseous membrane of the forearm, resulting in elbow restriction and dislocation. Other hallmarks include hypertrophic callus formation and a radiodense metaphyseal band of the long bones invariably seen in younger patients. On histological examination, a characteristic mesh-like pattern of lamellation is seen with polarized light microscopy. The causative gene remained unknown until recently. However, two groups have identified a single recurrent heterozygous mutation of c.-14C > T in the 5′-UTR of the gene encoding interferon-induced transmembrane protein 5 (*IFITM5*) in several families transmitted with complete co-segregation [Cho et al., 2012; Semler et al., 2012]. We report here the clinical and radiological manifestations in two affected individuals with the recurrent mutation.

Patient 1: A 5-year-old Japanese boy, was the first child of nonconsanguineous healthy parents. He was born at term after uneventful pregnancy and delivery. Birth weight, length, and OFC were 2,300 g (below 3rd centile), 46.9 cm (3rd–10th centile), and 32.0 cm (3rd–10th centile), respectively. At age 12 months, soon after he started walking, he suffered a fracture of the right tibia. Subsequently, fractures frequently occurred after mild trauma (four fractures between 1 and 4 years of age). He was referred for further assessment at age 4 years 10 months. His height was 96.8 cm (10th centile) and weight 13.0 kg (3rd–10th centile). The sclerae were white and dentition was normal. There was no joint laxity, skin hyperelasticity, or hearing impairment.

How to Cite this Article:
Takagi M, Sato S, Hara K, Tani C, Miyazaki O, Nishimura G, Hasegawa T. 2013. A recurrent mutation in the 5′-UTR of *IFITM5* causes osteogenesis imperfecta type V.
Am J Med Genet Part A 161A:1980–1982.

Radiological examination (Fig. 1A–F) showed generalized osteopenia and a narrow thorax with slender ribs. The ulnae appeared thin, and there was hyperostosis at the attachment of the interosseous membrane, radial bowing, and anteriorly dislocation of the proximal radii. Cortical hyperostosis was also noted at the lateral aspect of the proximal femoral shafts. The distal fibulae were medially bowed along with mild cortical thickening. Metaphyseal sclerosis of the long bones was evident particularly in the distal femur and distal radius. Calvarial wormian bones were not seen. The bone mineral density (BMD) of the lumbar spine (L2–L4) was

Conflict of interest: none.
Grant sponsor: Ministry of Health, Labour and Welfare of Japan; Grant number: Jitsuyoka (Nanbyo)—Ippan—014 23300102.
*Correspondence to:
Dr. Tomonobu Hasegawa, M.D., Ph.D., Department of Pediatrics, Keio University School of Medicine, 35 Shinanomachi, Shinjuku-ku, Tokyo 160-8582, Japan.
E-mail: thaseg@a6.keio.jp
Article first published online in Wiley Online Library (wileyonlinelibrary.com): 27 June 2013
DOI 10.1002/ajmg.a.36025

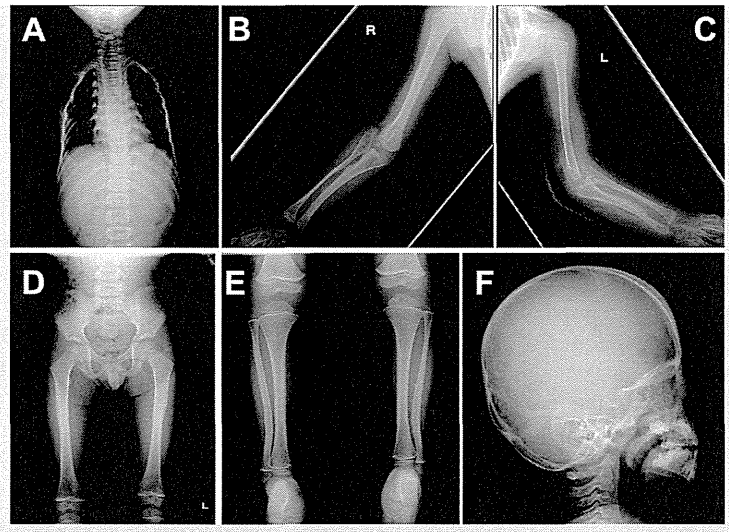

FIG. 1. Radiographs of Patient 1 at age 4 years 10 months. A: The thorax is narrow and ribs are slender. B,C: The ulnae appeared thin, and there is hyperostosis at the attachment of the interosseous membrane, radial bowing, and anteriorly dislocation of the proximal radii. Metaphyseal sclerosis is evident in the distal radii. D,E: Cortical hyperostosis is noted at the lateral aspect of the proximal femoral shafts. The distal fibulae are medially bowed along with mild cortical thickening. Metaphyseal sclerosis of the long bones was evident particularly in the distal femur. F: Calvarial wormian bones are not seen.

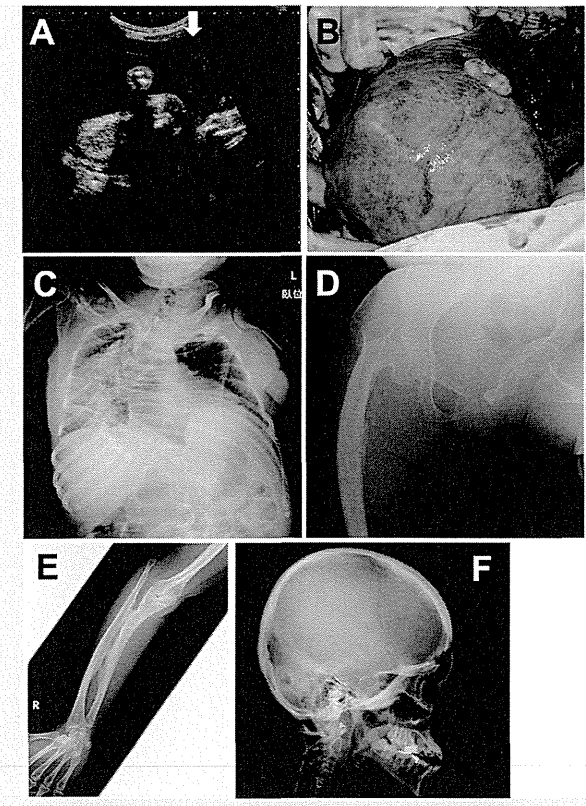

0.383 gm/cm^2 (Z-score of −3.4) (we used BMD reference data [del Rio et al., 1994] in Spanish children). Pamidronate treatment was initiated.

Patient 2: A 30-year-old Japanese woman, was born to healthy parents. The details of the clinical course in childhood were not available. She was said to have experienced the first fracture at age 7 years, and then suffered over 20 fractures, some of which required surgical correction. She developed progressive deformities of the extremities and scoliosis, and was consequently wheelchair bound. Adult height was 142.0 cm (below 3rd centile). She had white sclerae and normal dentition. She had no hearing impairment. At age 28 years, she gave birth to her first healthy child at 30 weeks of gestation by cesarean. The baby was a girl with birth weight of 1,332 g (appropriate for gestational age). The delivery was

FIG. 2. Ultrasonography and postpartum radiological examination of Patient 2. A: Ultrasonography at 28 weeks of gestation. Note a focal thinning and bulging at the upper segment of uterine wall (arrow). B: The head of the fetus is visible through the thin, almost transparent uterine wall. C–F: Postpartum radiological examination of Patient 2. C,D: Note severe thoracic scoliosis with thin ribs, acetabular protrusion, and generalized osteopenia of the axial skeleton. The tubular bones are slim along with metaphyseal osteopenia and diaphyseal cortical thickening. E: Abnormal ossifications are seen at the radioulnar interosseous membrane with proximal radial dislocation. Hyperostosis is noted at the medial aspect of the proximal radial shafts. F: No wormian bones are found.

complicated by incomplete uterine rupture. Ultrasonography at 28 weeks of gestation had shown a focal thinning and bulging at the upper segment of uterine wall (Fig. 2A). During the cesarean, the head of the fetus was visible through the thin, almost transparent uterine wall (Fig. 2B).

Postpartum radiological examination in the mother (Fig. 2C–F) demonstrated severe thoracic scoliosis with thin ribs, acetabular protrusion, and generalized osteopenia of the axial skeleton. The tubular bones were slim along with metaphyseal osteopenia and diaphyseal cortical thickening. Abnormal ossifications were seen at the radioulnar interosseous membrane with proximal radial dislocation. Hyperostosis was also noted at the medial aspect of the proximal radial shafts. No wormian bones were found. Quantitative heel ultrasound (QUS) showed her reduced bone quality (Z-score of −4.01, as measured by Speed of Sound).

After genetic counseling, we obtained written informed consent from the patient or parents for molecular studies, which were approved by the Institutional Review Board of the Keio University School of Medicine. Genomic DNAs were extracted from peripheral blood of the patients and parents by using standard techniques. We analyzed all coding exons and flanking introns of *IFITM5*, *COL1A1*, *COL1A2*, *LEPRE1*, *CRTAP*, *PPIB*, *FKBP10*, *SERPINF1*, *SERPINH1*, and *SP7* by using PCR and direct sequencing. Deletion or duplication involving *COL1A1* and *COL1A2* was checked by multiplex ligation-dependent probe amplification (MLPA) analyses (SALSA MLPA KIT P271, P272; MRC-Holland, Amsterdam, The Netherlands). We found a recurrent c.-14C > T mutation in the 5′-UTR of *IFITM5* in both patients. The mutation in Patient 1 was confirmed to be de novo. Other molecular analyses yielded normal results.

In conclusion, we validated the recently reported association between OI-V and the recurrent *IFITM5* mutation. However, further investigation is required to ascertain if the mutation is the exclusive cause of OI-V. Apart from the presence of hyperostosis, the skeletal manifestations in Patient 1 were mild to moderate, while those in Patient 2 were severe. The condition warrants a guarded prognosis because progressive bone deformity commonly ensues with age. It is important to note that the delivery in Patient 2 was complicated by uterine rupture despite absence of other extraosseous connective tissue abnormalities.

ACKNOWLEDGMENTS

We thank the patient and their families for participation in this study. This work was supported by a grant-in-aid for the Health Science Research Grant for Research on Applying Health Technology (Jitsuyoka [Nanbyo]-Ippan-014[23300102]) from the Ministry of Health, Labor and Welfare of Japan.

REFERENCES

Cho TJ, Lee KE, Lee SK, Song SJ, Kim KJ, Jeon D, Lee G, Kim HN, Lee HR, Eom HH, Lee ZH, Kim OH, Park WY, Park SS, Ikegawa S, Yoo WJ, Choi IH, Kim JW. 2012. A Single recurrent mutation in the 5′-UTR of *IFITM5* causes osteogenesis imperfecta type V. Am J Hum Genet 91: 343–348.

del Rio L, Carrascosa A, Pons F, Gusinyé M, Yeste D, Domenech FM. 1994. Bone mineral density of the lumbar spine in white Mediterranean Spanish children and adolescents: Changes related to age, sex, and puberty. Pediatr Res 35:362–366.

Forlino A, Cabral WA, Barnes AM, Marini JC. 2011. New perspectives on osteogenesis imperfecta. Nat Rev Endocrinol 7:540–557.

Glorieux FH, Rauch F, Plotkin H, Ward L, Travers R, Roughley P, Lalic L, Glorieux DF, Fassier F, Bishop NJ. 2000. Type V osteogenesis imperfecta: A new form of brittle bone disease. J Bone Miner Res 15:1650–1658.

Semler O, Garbes L, Keupp K, Swan D, Zimmermann K, Becker J, Iden S, Wirth B, Eysel P, Koerber F, Schoenau E, Bohlander SK, Wollnik B, Netzer C. 2012. A mutation in the 5′-UTR of IFITM5 creates an in-frame start codon and causes autosomal-dominant osteogenesis imperfecta type V with hyperplastic callus. Am J Hum Genet 91:349–357.

Endocrine Journal 2013, **60** (12), 1281-1287

ORIGINAL

Antenatal management of recurrent fetal goitrous hyperthyroidism associated with fetal cardiac failure in a pregnant woman with persistent high levels of thyroid-stimulating hormone receptor antibody after ablative therapy

Tadashi Matsumoto[1], Kei Miyakoshi[1], Yoshifumi Saisho[2], Tomohiro Ishii[3], Satoru Ikenoue[1], Yoshifumi Kasuga[1], Ikuko Kadohira[1], Seiji Sato[1], Naoko Momotani[4], Kazuhiro Minegishi[1] and Yasunori Yoshimura[1]

[1]*Department of Obstetrics and Gynecology, Keio University, School of Medicine, Tokyo 160-8582, Japan*
[2]*Department of Internal Medicine, Keio University, School of Medicine, Tokyo 160-8582, Japan*
[3]*Department of Pediatrics, Keio University, School of Medicine, Tokyo 160-8582, Japan*
[4]*Department of Endocrinology, Tokyo Health Service Association, Tokyo 162-8402, Japan*

Abstract. High titer of maternal thyroid-stimulating hormone receptor antibody (TRAb) in patients with Graves' disease could cause fetal hyperthyroidism during pregnancy. Clinical features of fetal hyperthyroidism include tachycardia, goiter, growth restriction, advanced bone maturation, cardiomegaly, and fetal death. The recognition and treatment of fetal hyperthyroidism are believed to be important to optimize growth and intellectual development in affected fetuses. We herein report a case of fetal treatment in two successive siblings showing *in utero* hyperthyroid status in a woman with a history of ablative treatment for Graves' disease. The fetuses were considered in hyperthyroid status based on high levels of maternal TRAb, a goiter, and persistent tachycardia. In particular, cardiac failure was observed in the second fetus. With intrauterine treatment using potassium iodine and propylthiouracil, fetal cardiac function improved. A high level of TRAb was detected in the both neonates. To the best of our knowledge, this is the first report on the changes of fetal cardiac function in response to fetal treatment in two siblings showing *in utero* hyperthyroid status. This case report illustrates the impact of prenatal medication via the maternal circulation for fetal hyperthyroidism and cardiac failure.

Key words: Graves' disease, Fetal hyperthyroidism, Fetal goiter, Prenatal diagnosis, Fetal therapy

ANTIBODIES to the thyroid-stimulating hormone receptor (TRAb) , like other IgG, do not cross the placenta until 16 weeks and, therefore, could not play a role in early thyroid embryogenesis [1]. However, after 17 weeks gestation, since TRAb cross the placenta and fetal thyroid gland also develops, patients with Graves' disease showing high titer of TRAb might have adverse impact on fetal and neonatal outcomes including hyperthyroidism, non-immune fetal hydrops, and growth restriction [2]. We herein described a case of successful management of fetal cardiac failure complicated by fetal goitrous hyperthyroidism associated with persistent high levels of maternal TRAb in a pregnant woman with Graves' disease in hypothyroid status treated with thyroid hormone replacement after subtotal thyroidectomy and radioiodine therapy. Our experience would be significant information on perinatal management in women with Graves' disease presenting high levels of TRAb.

Submitted Jun. 13, 2013; Accepted Aug. 12, 2013 as EJ13-0248
Released online in J-STAGE as advance publication Sep. 11, 2013

Correspondence to: Tadashi Matsumoto, M.D., Department of Obstetrics and Gynecology, Keio University, School of Medicine, 35 Shinanomachi, Shinjuku-ku, Tokyo 160-8582, Japan.
E-mail: tmatsumoto@a2.keio.jp

Materials and Methods

Measurements of thyroid hormone and TRAb

TSH, free T4 (fT4), and free T3 (fT3) were measured using an electro chemiluminescence immunoassay (ECLIA) with the Cobas ECLIA kits (Roche Diagnostics, Japan). The values were interpreted according to gestational or postnatal age [3]. TRAb were measured

by ECLIA with third-generation assay using anti TSH receptor monoclonal antibody (M22) (Elecsys anti-TSH receptor assay (Roche Diagnostics GmbH, Penzberg, Germany)) [4]. A positive result was defined as an antibody titer greater than or equal to 2.0 IU/L.

Assessment of fetal cardiac function

ACUSON Antares (Siemens Medical Solutions, Mountain View, CA, USA) ultrasound system equipped with a CH6-2 transducer (2-6 MHz) was used to evaluate fetal cardiac function. M-mode sonography or cardiotocography tracings were used commonly to measure baseline fetal heart rate. Current international guidelines recommend for the normal fetal heart rate baseline different ranges of 110 to 160 bpm. If the baseline rate is greater than 160 bpm, it is termed tachycardia [5]. The preload indexes (PLIs) and cardiothoracic area ratios (CTARs) were analyzed on the second fetus showing *in utero* hyperthyroid status. CTARs was defined as the ratio of the cardiac area to the thoracic area in the four-chamber view of the heart in diastole [6]. Less than 35 % CTAR is normal regardless of gestational age, whereas cardiomegaly was defined as CTAR greater than or equal to 35 %. The inferior vena cava (IVC) waveform of human fetuses has a pulsatile pattern comprising 3 phases, namely, reversed flow during atrial contraction (A), early forward flow coinciding with atrial diastole and ventricular systole (Sf), and late forward flow coinciding with ventricular diastole (Df). The PLIs-IVC is the ratio of the peak velocity of A to the peak velocity of Sf, and the value of this parameter increases under high preload conditions. In normal fetuses, PLIs-IVC values range from 0 to 0.37 and have no relation with gestational age [7].

Case Report

A 30-year-old-Japanese woman, gravida 1, para 0, was referred to the high-risk prenatal care unit in our hospital because of fetal tachycardia at 23 weeks of gestation. Obstetric ultrasound examination revealed an anterior fetal neck mass, which was bilobed, symmetrical, solid, and measuring 17 × 9 mm (Fig. 1). The fetal heart rate was around 170 bpm. No other structural abnormalities were noted and the amniotic fluid volume was within normal range. The mother had a history of Graves' disease and received medical therapy, followed by subtotal thyroidectomy and radioiodine therapy. As a result of those treatments, she developed hypothyroidism and levothyroxine (LT4) replacement was started. Until the mid-second trimester, she had been euthyroid with LT4 replacement therapy, although high titer of TRAb persisted. It was noted that she showed marked bilateral periorbital edema and exophthalmos. Her thyroid functions at 23 weeks of gestation were as follows: TRAb 381 IU/L [manufacture reference range: <2.0 IU/L], TSH 0.09 μU/mL [manufacture reference range: 0.3-4.5 μU/mL], free thyroxine (fT4) 1.7 ng/dL [manufacture reference range: 0.7-1.8 ng/dL], free triiodothyronine (fT3) 2.7 pg/mL [manufacture reference range: 2.0-4.5 pg/mL] (Table 1a). Based on these clinical findings, the fetus was diagnosed as having hyper-

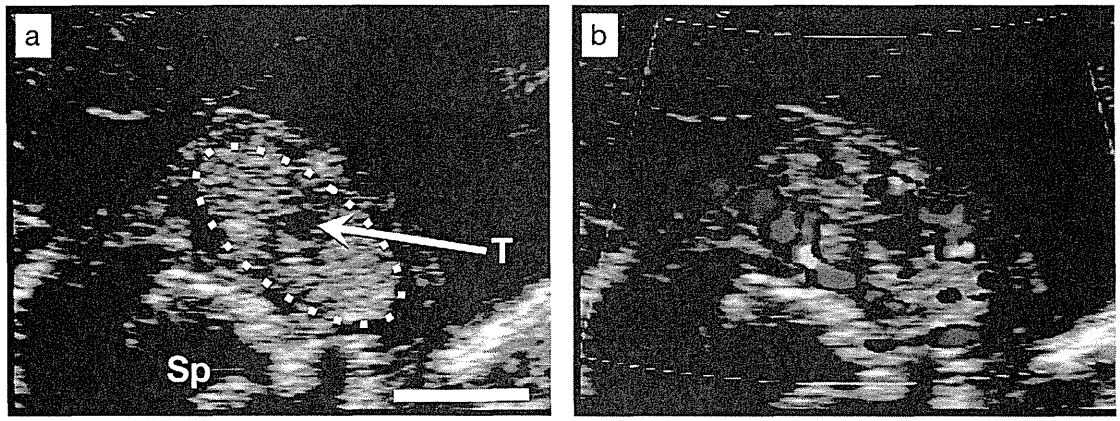

Fig. 1 Sonographic features of a fetal goitor
a. Transverse view of the fetal neck at 23 weeks gestation showing the thyroid mass located within the region of the ellipse. The trachea (T) is shown in the middle of the mass. Sp=spine. Bar=10mm
b. Color-flow Doppler imaging demonstrating the mass surrounded by abundant blood flow.

thyroidism. Because she had a history of eruption with use of methimazole (MMI), oral maternal potassium iodide (KI) (50 mg/day) and propylthiouracil (PTU: 150 mg/day) was initiated as *in utero* treatment for fetal hyperthyroidism. Since fetal heart rate didn't dropped and remained between 160 and 180 bpm, the dosage of PTU gradually increased up to 300mg at 34 weeks of gestation. During the follow-up, fetal growth restriction, defined as sonographic estimated fetal weight < -1.5 SD, became remarkable as pregnancy progressed, however, fetus did not develop cardiac failure and the heart rate was within normal range (141 bpm) after 35 weeks of gestation. At 36 weeks of gestation, a male neonate weighing 1,966 g was delivered by cesarean section because of possible dystocia due to enlarged fetal thyroid gland and non-reassuring fetal status. His Apgar scores at 1 min and 5 min were 8 and 9, respectively. On the day of birth, his thyroid gland was obviously enlarged and blood examination showed suppressed level of TSH (TRAb 445.0 IU/L [normal: <2.0IU/L], TSH 0.01 μU/mL [normal: 1.0-20.0 μU/mL], fT4 0.9 ng/dL [normal: 2.0-5.0 ng/dL], fT3 4.3 pg/mL [normal: 2.0-6.1 pg/mL], TSAb 2470 % [normal: <180 %]) (Table 1b) [reference ranges for neo-

Table 1a Maternal Thyroid Status

	Gestational weeks	TRAb [IU/L] (<2.0)	TSH [μU/mL]	fT4 [ng/dL] (0.7-1.8)	fT3 [pg/mL] (2.0-4.5)	Maternal treatment (/day)		
						LT4	PTU	KI
1st pregnancy	pre gestation	–	4.40 (0.3-4.5)	1.00	–	100μg	–	–
	23	381.0	0.09 (0.2-3.0)	1.7	2.7	150μg	150mg	50mg
	36	397.0	1.07 (0.3-3.0)	1.3	2.1	150μg	300mg	50mg
	postpartum 1 month	424.0	0.21 (0.3-4.5)	1.5	3.2	100μg	–	–
2nd pregnancy	pre gestation	230.0	4.16 (0.3-4.5)	1.7	1.8	100μg	–	–
	10	230.0	0.09 (0.1-2.5)	1.7	2.7	150μg	–	–
	21	223.0	0.10 (0.2-3.0)	1.8	3.6	150μg	300mg	50mg
	34	221.0	1.92 (0.3-3.0)	1.5	2.3	150μg	300mg	100mg
	postpartum 1 month	223.0	0.30 (0.3-4.5)	1.9	3.5	100μg	–	–

Normal range is shown in parenthesis.
The mother having a history of Graves' disease and received medical therapy was euthyroid status with levothyroxine replacement therapy, however, high titer of TRAb was persisted through two times of gestational period. TSH, thyroid-stimulating hormone (thyrotropin); TRAb, TSH receptor antibody; fT4, free thyroxine; fT3, free triodothyronine; LT4, levothyroxine; PTU, propylthiouracil; KI, potassium iodide

Table 1b Neonatal Thyroid Statuses

	thyroid status of each sibling	TRAb [IU/L]	TSH [μU/mL]	fT4 [ng/dL]	fT3 [pg/mL]
1st pregnancy	day 0	445.0 (<2.0)	0.01 (1.0-20.0)	0.9 (2.0-5.0)	4.3 (2.0-6.1)
	day 36	–	<0.01 (0.5-6.5)	0.8 (0.9-2.2)	3.8 (2.4-5.6)
	2 years	<0.3 (<2.0)	0.23 (0.5-4.5)	1.1 (0.7-2.0)	3.2 (2.3-6.6)
2nd pregnancy	day 0	120.0 (<2.0)	0.01 (1.0-20.0)	1.4 (2.0-5.0)	4.9 (2.0-6.1)
	day 15	–	<0.01 (0.5-6.5)	0.7 (0.9-2.2)	4.2 (2.4-5.6)
	8 months	0.6 (<2.0)	<0.01 (0.5-4.5)	1.7 (0.7-2.0)	4.0 (2.3-6.6)

Normal range is shown in parenthesis.
Laboratory examination of both neonates showed hyperthyroid status, and MMI was initiated immediately after birth. Levothyroxine replacement was implemented on Day 36 of 1st neonates and on Day 15 of 2nd neonates because the neonates showed central hypothyroidism. TSH, thyroid-stimulating hormone (thyrotropin); TRAb, TSH receptor antibody; fT4, free thyroxine; fT3, free triodothyronine